



Published in final edited form as:

Biomed Pharmacother. 2017 March ; 87: 58–72. doi:10.1016/j.biopha.2016.12.083.

Radiolabeled bombesin derivatives for preclinical oncological imaging

Carolina de Aguiar Ferreira^{a,1}, Leonardo Lima Fuscaldi^{b,1}, Danyelle M. Townsend^c, Domenico Rubello^{d,*}, and André Luís Branco de Barros^b

^aBiomedical Engineering Program, University of Wisconsin-Madison, Madison, WI 53705, USA

^bFaculty of Pharmacy, Federal University of Minas Gerais, Av. Antônio Carlos, 6627, 31270-901, Belo Horizonte, Minas Gerais, Brazil

^cDepartment of Drug Discovery and Pharmaceutical Sciences, Medical University of South Carolina, USA

^dDepartment of Nuclear Medicine, Radiology, NeuroRadiology, Medical Physics, Clinical Laboratory, Microbiology, Pathology, Santa Maria della Misericordia Hospital, Rovigo, Italy

Abstract

Despite efforts, cancer is still one of the leading causes of morbidity and mortality worldwide, with approximately 14 million new cases and 8.2 million cancer-related deaths each year, according to the World Health Organization. Among the strategies to reduce cancer progression and improving its management, implementing early detection technologies is crucial. Based on the fact that several types of cancer cells overexpress surface receptors, small molecule ligands, such as peptides, have been developed to allow tumor identification at earlier stages. Allied with imaging techniques such as PET and SPECT, radiolabeled peptides play a pivotal role in nuclear medicine. Bombesin, a peptide of 14 amino acids, is an amphibian homolog to the mammalian gastrin-releasing peptide (GRP), that has been extensively studied as a targeting ligand for diagnosis and therapy of GRP positive tumors, such as breast, pancreas, lungs and prostate cancers. In this context, herein we provide a review of reported bombesin derivatives radiolabeled with a multitude of radioactive isotopes for diagnostic purposes in the preclinical setting. Moreover, since animal models are highly relevant for assessing the potential of clinical translation of this radiopeptides, a brief report of the currently used GRP-positive tumor-bearing animal models is described.

Keywords

Radiolabeled bombesin derivatives; Molecular imaging; Oncological imaging; SPECT imaging; PET imaging; Preclinical data

*Corresponding author. domenico.rubello@libero.it, rubello.domenico@azisanrovigo.it (D. Rubello).

¹These authors contributed equally to the writing of this article.

Conflict of interest

None.

1. Introduction

Nuclear Medicine is a medical subspecialty that employs radiopharmaceuticals for molecular imaging purposes and allows clinicians to visualize the spatial and temporal changes within target tissues *in situ*. Images are generated from gamma emitters, Single Photon Emission Computed Tomography (SPECT), or positron emitters, and Positron Emission Tomography (PET). These modalities may be associated with anatomical imaging approaches, such as Computed Tomography (CT) or Magnetic Resonance Imaging (MRI), in order to confer spatial resolution [1,2].

Radiopharmaceuticals are administered to patients and circulate through the body, accumulating in the target organ or tissue of specific interest. Once in the target tissue, radiopharmaceuticals do not interfere with cell physiology, reflecting processes without any change. Therefore, SPECT and PET are molecular imaging modalities that can be used for visualization, characterization and measurement of biological events at the molecular level. Consequently, these molecular imaging modalities have the power to detect premature tissue alterations leading to an earlier and more accurate diagnosis and consequently better treatment options that lead to higher cure rates. In addition to diagnosis, these imaging modalities are able to characterize and stage primary tumors, as well as identify metastases in distant organs. Advantages posed by these techniques are powerful in that they permit follow-up tumor progression or recurrence, contributing to the choice of the best treatment regimen [6,7]. On the other hand, conventional imaging techniques, such as Ultrasonography, X-ray, CT and MRI, require anatomical and morphological organ alterations which occur at later stages of the disease, hence detection occurs in more advanced stages [3–5].

It is also important to consider that several physiological processes are pathologically upregulated in cancer cells when compared to normal cells. Therefore, the physiological processes that are dysregulated could be utilized as a target for molecular imaging in order to differentiate tumor from normal tissues. For example, several peptide receptors have been identified as overexpressed components on tumor cells surface when compared to their expression in normal cells (Table 1). Thus, many peptides and their derivatives have been radiolabeled and investigated as potential cancer diagnostic agents for molecular imaging by SPECT and PET [8–11].

Peptide molecules that are suitable for imaging techniques consist of up to 50 amino acid residues, with low molecular weight. Consequently, they readily diffuse into tumor tissue and have fast blood clearance, leading to improved imaging with less background. Furthermore, the peptides present low antigenicity, as well as high metabolic stability and tolerance towards molecular modifications due to the radiolabeling procedure. Therefore, radiolabeled peptides have been extensively investigated as molecular imaging probes for tumor detection over the last years [12,13].

Despite intense research in this field, only a few radiopeptides have emerged from preclinical studies to clinical trials, in order to assess their real potential for accurate and early cancer detection. In fact, at present the literature reports only a radiolabeled somatostatin derivative (^{111}In -Octreoscan or $^{99\text{m}}\text{Tc}$ -Octreoscan) has been approved and is

available as a radiopharmaceutical for neuroendocrine cancer diagnosis in Nuclear Medicine [8,14]. However, radiolabeled peptides specific to tumor tissue are an important strategy for cancer diagnosis and patient follow-up by SPECT and PET modalities.

2. Bombesin

The neuropeptide Bombesin (BBN) was primarily isolated from the skin of the European fire-bellied toad, *Bombina orientalis*. The peptide is composed of 14 amino acid residues and carries a natural carboxyl-terminal (C-terminal) carboxamide. It is homolog to the mammalian gastrin-releasing peptide (GRP), exhibiting high similarity in their C-terminal portion (Table 2) [15].

Bombesin binds to and activates G-protein coupled receptors, known as gastrin releasing peptide receptor (GRPR). Four BBN receptor subtypes have been described to-date: neuromedin B receptor (BB1r), gastrin-releasing peptide receptor (BB2r or GRPr), orphan receptor (BB3r), and amphibious receptor (BB4r). The latter is found in amphibians, while the others are presented in mammalian cells. They are all G-protein coupled receptors and their pharmacological activities include the stimulation of hormones releasing, like gastrin and somatostatin, as well as the stomach and intestine smooth muscle contraction. Furthermore, those BBN receptors expressed in cancer cells exhibit mitogenic effects, stimulating tumor cell proliferation when activated by agonistic molecules [16–18].

Several studies have used radiolabeled BBN derivatives in order to identify tumor cells. Both non-modified and truncated BBN sequences have been assessed and the truncated peptides present some advantages compared to the non-modified peptides. First, they are chemically synthesized with lower cost and time. Beyond that, the removal of amino acid residues increases *in vivo* stability, as well as biological half-life. Consequently, there is an increase in the biological half-life of the peptide, resulting in higher accumulation in tumor tissue [8]. As an example, it can be mentioned the truncated BBN sequence that contains the eight C-terminal amino acid residues, named BBN₍₇₋₁₄₎. The removal of the six nitrogen-terminal (N-terminal) amino acid residues of BBN increases its stability and maintains peptide affinity for the binding site on the receptor [19]. It is also important to highlight that agonistic BBN derivatives bind to BBN receptors expressed on cancer cells surface where they are subsequently internalized into the cytoplasm. On the other hand, antagonistic BBN derivatives do not exhibit this feature. Therefore, agonistic BBN molecules accumulate in higher amounts in tumor tissues and are more suitable as oncological diagnostic agents [20].

Advanced *in vitro* and *in vivo* studies have been performed in order to assess the real potential of radiolabeled BBN derivatives as tumor imaging probes. Although promising preclinical data have been achieved, radiolabeled BBN derivatives are not presently approved and commercially available radiopharmaceutical. Hence there are a limited number of clinical trials, as well as the few number of evaluated patients [8]. Despite promising clinical results, more extensive clinical trials are necessary in order to establish radiolabeled BBN derivatives as oncological molecular imaging probes. Therefore, the present revision intends to summarize the most important radiolabeled BBN derivatives preclinical data.

3. Tumors overexpressing bombesin receptors and animal models

Cancer is one of the most important causes of morbidity and mortality worldwide. Global data revealed more than 14 million new cases of this disease in 2012, followed by more than 8 million deaths [21], most of which might be avoided if an early diagnosis could be achieved, leading to better prognostics. Some types of cancer cells, such as breast, colon, lung, pancreas and prostate, exhibit upregulation of BBN receptor expression, specifically subtype BB2r or GRPr [14,22]. These tumors are among the most prevalent cancer, being the leading cause of death by this malignancy, and a variety of human cancer cell lines have been demonstrated to overexpress BBN receptor, such as MCF7, MDA-MB-231, T-47D, BT474 (breast cancer); HT-29 (colorectal cancer); A427, A549 (lung cancer); Capan-1 (pancreatic cancer); DU 145; LNCaP; PC-3; 22Rv1 (prostate cancer). Therefore, GRPr might be a potential target for cancer diagnosis, using radiolabeled BBN derivatives as specific molecular imaging probes for these types of cancers.

Animal model systems are highly important to assess the potential of new radiopeptides, including BBN derivatives, as molecular imaging probes for cancer diagnosis, because biochemical and cellular assays often do not reflect *in vivo* conditions, and clinical trials are initially limited by cost, time and ethical constraints. In this sense, in experimental oncological studies, several animal models have been evaluated in the attempt to better represent the disease as it occurs in humans [23–25]. The important issues related to oncological animal models are concerning to the type and the site of tumor cells inoculation using allograft or xenograft model systems. The former is obtained by the inoculation of tumor cells from the own animal species used while xenograft models are developed by the inoculation of tumor cells from other species, such as human tumor cells [23–25]. Both allograft and xenograft tumor models have been used for the development of radiolabeled BBN derivatives, specifically the inoculation of Ehrlich cells (murine breast cancer cells) in Swiss mice (allograft model) [26,27], and the inoculation of MDA-MB-231 cells (human breast cancer cells) in athymic nu/nu mice (xenograft model) [28]. It is important to mention that xenograft inoculation requires the use of immune-compromised animals, such as nude mice (T-cells deficiency) and severe combined immunodeficiency (SCID) mice (T-and B-cells deficiency), in order to avoid cancer cells rejection and to assure tumors development. Although these immune-compromised animals need special care, such as sterile cages with autoclaved wood shavings, food and water, as well as special shelves with filtered air, xenograft models are the most used in oncological animal experimentation, since several of human cells exhibit high expression of BBN receptors [23–25].

The second important consideration is the location of tumor seeding which can be orthotopic or ectopic. Orthotopic models are a result of tumor cells inoculation directly in the corresponding organ, such as prostate tumor cells inoculated in the animal's prostate. However, orthotopic inoculation presents some disadvantages, including the inability to following tumor development without additional fluorescent tracers and the need for a consolidated domain of the inoculation technique. On the other hand, ectopic models consist of tumor cells inoculation at a different site, like a subcutaneous inoculation of prostate cancer cells. This strategy is easier and less invasive, as well as it allows following tumor development and measuring tumor size *in vivo* [23–25]. However this has the clear

disadvantage of not forming tumors in the organ of tumor origin and complexity of the microenvironment.

Finally, it is important to mention that *in vivo* data may differ from species to species, and may have gender differences that bias interpretation [8]. Moreover, animal models clearly do not represent the exact reality in humans. Therefore, experimental model limitations are unavoidable. However, the selection of a suitable oncological animal model associated with careful data analysis provides relevant information concerning to new radio-peptides, such as radiolabeled BBN derivatives. A summary of several oncological animal models, used for the evaluation of radiolabeled BBN derivatives as imaging probes, are presented in Table 3.

4. Radiolabeled BBN derivatives in preclinical studies

The overexpression of Bombesin receptors in multiple tumor types, often which have a poor prognosis in patients with extensive disease, has led to considerable interest in the drug development as well as imaging modalities [17]. Radiolabeled peptides for targeted cancer therapy/imaging are one of the largest groups of radiopharmaceuticals currently researched. These moieties are built of a targeting peptide, such as Bombesin, that binds *in vivo* to a specific receptor overexpressed in cancer cells and a radioisotope that allows localization of the tumor by SPECT or PET Imaging. Often a linker or bifunctional chelator (BFC) is used to form a stable complex.

The advantages of using peptides for targeted radioimaging are favorable tissue distribution, fast clearance, low immunogenicity and inexpensive, automated production [29]. In nuclear medicine for diagnostic purposes, important factors to consider are half-life, mode of decay, cost and availability of the radionuclide. The half-life of the radionuclide should allow sufficient uptake and distribution to yield considerable contrast and quality images. The radionuclide emission energies should be appropriate for proper detection by the equipment, while cost and availability are also important considerations [30]. Several radioisotopes are used currently for SPECT imaging, such as ^{99m}Tc , ^{123}I , ^{67}Ga and ^{111}In , as well as for PET imaging, including ^{18}F , ^{11}C , ^{64}Cu , and ^{68}Ga , among others [31]. Each isotope has their own properties that must be considered during the preparation of the radiopharmaceutical to achieve better outcomes.

4.1. Technetium-99m

The vital role of Tc-99m (^{99m}Tc) in the field of diagnostic nuclear medicine is well established and as such there is great interest in developing radiopharmaceuticals utilizing PET isotopes because of better sensitivity and resolution. The importance and prominence of ^{99m}Tc is due to its optimal nuclear properties (single 140 keV gamma photon emission and relatively short half-life of 6.02 h) and ability to form stable complexes with a variety of chelating agents under mild conditions [32]. In addition, the radioisotope is readily obtained in the form of pertechnetate directly from $^{99}\text{Mo}/^{99m}\text{Tc}$ generators on elution with physiologic saline [33]. These facts altogether make ^{99m}Tc an ideal radioisotope for SPECT imaging, since it allows rapid data collecting scanning procedures while maintaining total patient radiation exposure in lower values with a relatively inexpensive isotope cost. The radiochemical characteristics of ^{99m}Tc are especially suitable for tumor-specific

radiopharmaceuticals that have biological half-lives well-matching the time-course of tumor uptake and the background clearance of the radiolabeled tumor-targeting biomolecules, such as bombesin-like peptides [34]. Bifunctional chelating agents such as MAG3, N2S2, tripeptide triamino-thiol (N3S), S4, P2S2, DTPA, 2-picolylamine-*N,N*-diacetate and the α -histidinyl acetatecarbonyl have been used for stabilization of the radioactive metal center under *in vivo* conditions. Other chelators have also been proposed to conjugate ^{99m}Tc to active biological components, such as PNP and HYNIC [35]. In this context, many studies utilizing ^{99m}Tc labeled-bombesin have been described and a summary can be found in Table 4.

In 1998, Baidoo et al. [36] was the first to describe the first use of ^{99m}Tc as the radioisotope for Bombesin analog radiolabeling. In that study, two different diaminedithiol (DADT) based linkers were used (Hx-DADT and Pm-DADT) to conjugate the radioisotope into a full-length bombesin peptide. *In vitro* binding assay using rat brain membranes endorsed the high affinity of both designed radiopeptides in a similar level as found for natural bombesin. Biodistribution studies in normal mice revealed that the Hx-DADT chelator, due to its more lipophilic character, increase 4-fold the intestine uptake, in comparison to the radiolabeled complex containing Pm-DADT. The authors conclude that not only ^{99m}Tc -Pm-DADT-[Lys3]BBN is a more suitable agent for abdominal area imaging but also that ^{99m}Tc is a valuable radioisotope for Bombesin analogs radiolabeling, paving the way for the development of ^{99m}Tc -labeled Bombesin peptides.

Faintuch et al., after describing the radiolabeling methods of $\text{BBN}_{(7-14)}$ with ^{99m}Tc using hydrazinonicotinic acid (HYNIC) as a bifunctional chelator [37], reported detailed *in vitro* and *in vivo* comparative studies between ^{99m}Tc -HYNIC-BBN and ^{99m}TcN (PNP6)-Cys-BBN [38]. Scintigraphic images performed after injection of ^{99m}Tc -HYNIC-BBN in nude mice transplanted with prostate cancer cells demonstrated significant tumor uptake, as demonstrated in Fig. 1. Tumor uptake of ^{99m}Tc -HYNIC-BBN was higher than that of ^{99m}TcN (PNP6)-Cys-BBN, indicating that the chelator type influences *in vivo* pharmacodynamics properties. Blocking experiments were also performed through co-injection of excess BBN resulting in significant reduction in the radiopeptide uptake in liver, pancreas and tumor.

Using HYNIC as a bifunctional chelating ligand, de Barros et al. [39] radiolabeled, in the presence of EDDA as a co-ligand, $\text{BBN}_{(7-14)}$ with ^{99m}Tc . Using Ehrlick tumor-bearing Swiss mice, they evaluated its potential as a tumor identification tool through biodistribution and scintigraphics. Although tumor uptake was relatively low in terms of% of injected dose per gram (up to 0.87% ID/g), the radioactive compound exhibited high tumor-to-muscle ratio (up to 6 at 480 min post-injection) [39]. Interestingly, the same research group developed a freeze-dried kit for labeling HYNIC- β -Ala- $\text{BBN}_{(7-14)}$ with ^{99m}Tc with high *in vitro* stability up to 180 days of storage, the efficacy of which was confirmed by biodistribution studies and scintigraphic images [22]. This constitutes a major advance in translating preclinical methods to the clinical use of radiopharmaceuticals since it simplifies the radiolabeling procedure and reduce radiation exposure during preparation while maintaining its stability and yielding high radiochemical purity at low cost [22].

Exploring the fact that Capan-1 tumor cell lines express functional GRPr on its membrane surface, Carlesso et al. [40] evaluated the feasibility of ^{99m}Tc HYNIC- β -Ala-BBN₍₇₋₁₄₎ to serve as an imaging agent for human pancreatic adenocarcinoma. Biodistribution studies confirmed the radiopeptide was excreted by the urinary tract and had higher tumor-to-muscle values in later times (4 h after injection) while kidney and bladder have lower radiation signals. All target/non-target ratios from scintigraphic images and *ex vivo* biodistribution assay were higher than 1.5, indicating that the formulated imaging agent is able to identify Capan-1 pancreatic adenocarcinoma [40]. ^{99m}Tc HYNIC- β -Ala-BBN₍₇₋₁₄₎ has also been successfully used in scintigraphic studies of other types of tumor models, such as human breast (MDA-MB-231 cells) [28] and colon (HT-29 cells) [41] cancer, in which tumor-to-muscle ratios were up to 6.00 (at 4 h post injection) and up to 11.17 (at 1 h post injection) respectively.

Liolios et al. [34] conducted an investigation of the influence of positively charged aminoacids as spacers between chelators and BBN peptide. Two BN-derivatives of the general structure [M-chelator]-(spacer)-BN₍₂₋₁₄₎-NH₂, where M: ^{99m}Tc or $^{185/187}\text{Re}$, chelator: Gly-Gly-Cys-, spacer: (arginine)₃-, M-BN-A; spacer: (ornithine)₃-, M-BN-O; were prepared and evaluated as tumor imaging agents. Scintigraphic images of PC-3 tumor-bearing mice showed that the tumor accumulation peak observed for ^{99m}Tc -BN-A was between 15 and 30 min post injection (6.94 ± 0.50 ; $3.40 \pm 1.17\% \text{ID/g}$), while for ^{99m}Tc -BN-O was between 60 and 120 min p.i. (7.14 ± 0.87 ; $7.92 \pm 0.79\% \text{ID/g}$). These studies concluded that ^{99m}Tc -BN-O maintained a high tumor uptake for a longer time period but with higher kidney accumulation, while ^{99m}Tc -BN-A presented lower kidney accumulation but was cleared faster from the body and from the tumor.

The first-in-man study of the application of ^{99m}Tc radiolabelled-BBN derivatives was carried out by Ananias et al. in 2013. In this study, the use of ^{99m}Tc -HYNIC(tricine/TPPTS)-Aca-Bombesin₍₇₋₁₄₎ for the detection of prostate cancer was considered to be safe but hindered by an unexpectedly low *in vivo* metabolic stability in man [42], demonstrating the need for further investigation of the poor correlation between preclinical studies in mouse tumor models with *in vivo* performance in cancer patients.

Scopinaro et al. [43] evaluated the ability of ^{99m}Tc -bombesin to detect prostate cancer and regional lymph node invasion in 10 patients (8 with primary prostate tumor and 2 with benign adenomas). The studies enrolled patients without cancer, patients with cancer but without node invasion, and patients with cancer and node invasion. All 8 primary tumors were visualized in the prostate fossa by SPECT while 2 patients with benign adenomas did not show uptake. In this study, SPECT showed uptake in obturator nodes that were proven to be cancer-specific after histopathology in 3 patients while MRI or CT did not show these LN metastases.

4.2. Gallium-68

Gallium-68 (^{68}Ga) is a positron-emitting radionuclide that, although first used in clinical medicine in the early 1960s [44], have only been progressively applied in nuclear imaging since $^{68}\text{Ge}/^{68}\text{Ga}$ generator systems have been commercially available resulting in a reliable, cost-effective and convenient method for its production and purification [45]. ^{68}Ga decays

89% through positron emission (maximum energy of 1.92 MeV, mean 0.89 MeV) and has a short physical half-life ($t_{1/2} = 68$ min) that enables improved dosimetry and repetitive imaging, making it ideal for clinical use. In addition, ^{68}Ga -based peptides are increasingly recognized as a new class of radiopharmaceuticals, showing very fast blood clearance and fast target localization [46]. Furthermore, ^{68}Ga -based radiotracers provide sufficient levels of radioactivity for high-quality images in a short scanning time, allowing repeat examinations on the same day and, in general, show better pharmacokinetics overall despite similar uptake in tumors [47].

A BBN analog, [DTyr⁶, β -Ala¹¹, Thi¹³, Nle¹⁴] BBN₍₆₋₁₄₎ also called BZH3, was radiolabeled with ^{68}Ga through DOTA-PEG₂ conjugation [48]. *In vivo*, high tumor-to-tissue ratios 1 h after injection and a rapid clearance of unbound peptide from GRPr-negative, normal tissues was observed. PET images obtained 1 h after injection demonstrated a clear delineation of the tumor tissue (up to 7.0%ID/g) and a low activity background in lungs, liver and circulation, demonstrating the diagnostic potential of ^{68}Ga -BZH3 in a prostate cancer xenograft mouse model. Moreover, the low liver uptake of 0.5%ID/g of ^{68}Ga -BZH3 versus 3–8%ID/g observed, in previously published papers [49–51], for $^{99\text{m}}\text{Tc}$ -labeled BBN analogs should facilitate tumor localization in the abdominal region when compared with $^{99\text{m}}\text{Tc}$ imaging. ^{68}Ga -BZH3 also appears to be much more favorable with regard to *in vivo* stability and biodistribution properties than described for $^{99\text{m}}\text{Tc}$ -labeled bombesin derivatives [48]. In 2007, the platform was modified by conjugating ^{68}Ga and ^{177}Lu with the 8-amino acid peptide bombesin [BBN₍₇₋₁₄₎] using DOTA-PEG₄ as a chelator [52]. Although the binding affinity of those complexes was relatively low, the radiopeptides showed higher tumor uptake (14.8%ID/g at 1h) and relatively slower washout from the tumor in comparison with previously published paper [52].

Liu et al. [53] investigated the dual receptor-targeting property and tumor diagnostic value of ^{68}Ga -labeled RGD-BBN against both the $\alpha_v\beta_3$ integrin and GRP receptors using a PC-3 tumor mouse model. MicroPET images showed that ^{68}Ga -NOTARGD-BBN had higher tumor uptake than ^{68}Ga -NOTARGD and ^{68}Ga -NOTA-BBN. These studies validated that ^{68}Ga -labeled RGD-BBN had a convenient synthesis method, high specific activity, increased tumor uptake and was able to image tumors with either integrin or GRPR expression.

A bombesin antagonist analog, [D-Phe⁶, Sta¹³, Leu¹⁴]-bombesin₍₆₋₁₄₎ (RM26) was synthesized and conjugated to NOTA *via* a PEG₂ linker and radiolabeled with ^{68}Ga and ^{111}In by Varasteh et al. [54]. Tumor targeting and biodistribution studies in PC-3 xenograft models displayed high and specific uptake in tumors ($8.1 \pm 0.4\%$ ID/g ^{111}In for ^{68}Ga and $5.7 \pm 0.3\%$ ID/g for ^{111}In) and favorable tumor-to-background ratios (tumor-to-blood: 12 ± 1 for ^{68}Ga and 10 ± 1 for ^{111}In) after only 1 h post injection [54]. Later, the same group evaluated if a variation of mini-PEG spacer length could improve the targeting properties of the NOTA-conjugated RM26 in PC-3 and BT-474 (breast cancer) xenograft model systems. High uptake in tumors ($4.6 \pm 0.6\%$ ID/g and $2.8 \pm 0.4\%$ ID/g for PC-3 and BT-474 xenografts, respectively) and high tumor-to-background ratios (tumor-to-blood of 44 ± 12 and 42 ± 5 for PC-3 and BT-474 xenografts, respectively) were found already at 2 h p.i.

of ^{68}Ga -NOTA-PEG3-RM26. Nonetheless, that influence is minor when di-, tri-, tetra- and hexaethylene glycol units are compared [55].

In more recent studies, Lim et al. [56] synthesized a DOTA-glu-BBN₍₇₋₁₄₎ analog radiolabeled with ^{68}Ga , performed PET-CT imaging studies in subcutaneously and peritoneal metastasized PC-3 prostate tumor mouse model and compared results to ^{18}F FDG. The tumor-to-muscle ratio of ^{68}Ga -DOTA-glu-BBN was 1.7-fold higher than that of ^{18}F FDG (4.79 for ^{18}F FDG and 7.96 for ^{68}Ga -DOTA-glu-BBN), and ^{68}Ga -DOTA-glu-BBN was excreted more rapidly from the blood pool than ^{18}F FDG. Considering ^{68}Ga -DOTA-glu-BBN, apart from the uptake of radioactivity in the peritoneal area, the tumor cells in the upper body was clearly imaged with low background radioactivity. However, the uptake of radioactivity in the pancreas could hinder efforts to detect tumors in the peritoneal cavity [56].

A novel bombesin analog, QWAV-Sar-H-FA01010-Tle-NH₂ (BBN2) was radiolabeled with ^{68}Ga using NOTA as linker [57]. The tumor-targeting property of ^{68}Ga -NOTA-BBN2 was studied in two different prostate cancer xenografts models (hormone-dependent LNCaP and hormone independent PC-3) with dynamic PET imaging. Results showed relatively high tumor-to-muscle ratios in both model systems (5.86 ± 0.37 for PC-3 and 5.79 ± 1.02 for LNCaP). Representative PET images of both tumors 1 h after injection of ^{68}Ga -NOTA-BBN2 can be found in Fig. 2. These studies also investigated the “serve-and-protect” strategy [58], by evaluating the influence of protease inhibitor phosphoramidon on metabolic stability and tumor uptake. However, even though the use of this concept have been applied to radiopeptides labeled with short-lived positron emitters [58], no increase of metabolic stability or tumor uptake was found [57]. Maecke et al. [59] summarized clinical studies of a GABA-[D-Tyr6,β-Ala11,Thi13,Nle14]BN(6-14), or BZH2, radiolabeled with ^{68}Ga . PET scans in 11 patients with prostate cancer were performed. Primary tumors were visible in all patients as well as lymph node metastases in three patients. Pancreatic uptake was seen in four patients and clearance was predominantly renal with >75%ID recovered in the urine at 60 min, Table 5.

4.3. Copper-64

Copper-64 (^{64}Cu) has a radioactive half-life of 12.7 h and decays to either ^{64}Ni by positron emission (β^+ = 17.9%, E_{max} = 660 keV, A_{average} = 288 keV) or electron capture (EC = 43.1%, E = 1675 and 1346 keV), or ^{64}Zn by β^- -decay (β^- = 39.0%, E = 190.2 keV) [60]. These properties indicate that ^{64}Cu has the potential to be used in diagnostic PET imaging and radiotherapeutic applications. The relatively long half-life concedes at least two main advantages: 1) the possibility to be produced at regional or nation cyclotron facilities and distributed to local nuclear medicine departments with the loss of approximately one half-life [61]; and 2) the possibility of enabling imaging at delayed time points, which allows sufficient time for clearance from background tissues, resulting in increased image contrast. This is particularly important for targeting molecules that demonstrate long circulation times, such as antibodies and nanoparticles [62]. Although the impracticability of being covalently incorporated into biological molecules, the well-established coordination chemistry of copper allows for its reaction with a wide variety of bi-functional chelator

systems that can be linked to antibodies, proteins, peptides and other biologically relevant small molecules [63].

Copper-64 has several unique attributes that make it a multipurpose radionuclide, combining diagnostic imaging and radiotherapy, known as theranostic applications. While the positron emission allows high-resolution images with no impairment from abundant gamma emissions, the combination of positron and beta-emission, as well as the emission of high LET Auger electrons, imparts a high local radiation dose and cytotoxic potency at the cellular level [64]. Copper cations (Cu^{+2}), if released *in vivo*, can bind to serum proteins like albumin and accumulate in non-targeted organs such as the liver. Therefore, the stability of Cu(II) complexes is an important parameter in radiopharmaceutical applications and, for that, chelators are commonly used. The most widely used chelators for attaching ^{64}Cu to biologic molecules are tetraazamacrocyclic ligands with pendant arms that utilize both the macrocyclic and chelate effects to enhance stability. Two of the most widely studied chelators are DOTA (1,4,7,10-tetraazacyclododecane-1,4,7,10-tetraacetic acid) and TETA (1,4,8,11-tetraazacyclotetradecane-1,4,8,11-tetraacetic acid)[61]. It is important to highlight that NOTA (1,4,7-triaza-cyclo-nonane-1,4,7-triacetic acid) and its derivatives are often chosen because of the high degree of stability of the formed complexes as well as the possibility of side-by-side comparisons of the same chelator-peptide conjugations but different radiometals [47].

In 2003, the first GRP receptor targeting radiopharmaceutical to be used for PET imaging through ^{64}Cu radiolabeling of the BBN analog was introduced by Rogers et al. [65]. These studies demonstrated that a BBN analog could be radiolabeled with the positron-emitter ^{64}Cu with high affinity. It was also found that the complex DOTA-Aoc-BBN₍₇₋₁₄₎ could internalize into GRPr positive cells and target GRPr positive tumors, as confirmed by micro-PET imaging and biodistribution studies. However, the liver and pancreas had significantly greater uptake ($P < 0.05$) than the tumor at all three time points studied. Additionally, normal tissue uptake was higher than other findings with different radioisotopes, resulting in a low tumor-to-non-tumor ratio. The same group then tested the hypothesis that the specificity of the complex ^{64}Cu -BBN could be improved by using PEG instead of Aoc (aminooctanoic acid). Results showed a significant reduction of the binding affinity to GRP receptor, a faster blood clearance and a reduce pancreatic uptake of DOTA-PEG-BBN₍₇₋₁₄₎ in comparison to DOTA-Aoc-BBN₍₇₋₁₄₎ [66]. Additional studies with different BBN analogs radiolabeled with ^{64}Cu have been reported and examples are summarized in Table 6.

Using DOTA as a linker, Chen et al. [67] evaluated the efficacy of radiolabeling of full-length BBN agonist (Lys³-BBN) in prostate cancer xenografts induced by PC-3 cells or androgen dependent CWR22 cells. Biodistribution studies indicated that the radiopeptide uptake was higher in PC-3 than in CWR22 xenografts. Furthermore, through microPET and autoradiography imaging, both tumor models showed a very high tumor-to-background ratio whereas pancreas and tumor accumulation was lower when compared to biodistribution studies. Yang et al. [68] examined the combination of which BBN analog (full-length or truncated), and which linker (DOTA or DOTA-Aoc) were more suitable for PET imaging purposes, using ^{64}Cu as the radioisotope. *In vitro* and *in vivo* data which included PET

imaging, showed that the full-length compound DOTA-[Lys3]BBN had higher binding affinity, internalization and retention rates as well as more stability in the tumor, blood and urine samples than DOTA-Aca-BBN₍₇₋₁₄₎ analog. Attempting to alter the pharmacokinetic parameters, Parry et al. [69] indicated that incorporation of specific hydrophilic amino acids into the conjugate framework was able to reduce background tissue uptake as compared to aliphatic linkers such as 8-Aoc. Uptake and retention of ⁶⁴Cu-DO3A-X-BBN₍₇₋₁₄₎NH₂ (X = GGG, GSG, GSS) in all tissues were still markedly high, indicating possible demetallation of Cu-64 from DOTA and trapping or complexing to proteins in specific tissues.

Nanda et al. [70] compared tumor-to-non-tumor uptake ratios of three Cu-BBN conjugates with different linkers (NOTA-6-Ahx, NOTA-8-Aoc and NOTA-9-Anc) and found ratios that were considerably high for some tissues (muscle and bone) both at 1 and 4 h p.i., whereas they were comparable to most other tissues, showing that diagnostically useful ratios could only be achieved after a delayed time point. Molecular imaging studies carried out 15 h post injection allowed clear visualization of PC-3 tumor tissue in xenograft models and the [⁶⁴Cu-(NO2A-6Ahx-D-Phe6-BBN₍₆₋₁₃₎NH₂)] conjugate exhibited the highest targeted accumulation in GRPR-expressing tissue as well as the most efficient clearance of radiotracer from whole-body tissue *via* the renal-urinary excretion pathway [70]. With the goal of improving tumor-to-normal tissue ratios, Craft et al. [71] conjugated BBN with p-SCN-Bn-NOTA for complexing ⁶⁴Cu. Although results showed rapid internalization of the complex into PC-3 cells and rapid tumor uptake, the tumor-to-normal tissue ratios for ⁶⁴Cu-NOTA-Bn-SCN-Aoc-BN₍₇₋₁₄₎ were similar to the ratios observed for ⁶⁴Cu-NO2A-Aoc-BN₍₇₋₁₄₎ at 1 and 4 h, but less at 24 h due to the rapid tumor clearance. Bergmann et al. [72] evaluated ⁶⁴Cu-labeled bombesin analogs featuring a bis (2-pyridylmethyl)-1,4, triazacyclononane chelator targeting properties in prostate cancer cells xenotransplanted in mice. Small animal PET imaging studies demonstrated a very high degree of tumor accumulation for ⁶⁴Cu-DMPTACN-βAla-βAla-BBN₍₇₋₁₄₎ and ⁶⁴Cu-DMPTACN-βhomoGlu-βAla-βAla. Incorporation of a single additional glutamic acid residue within the spacer between bombesin and the radiolabeled complex (⁶⁴Cu-DMPTACN-βhomoGlu-βAla-βAla-BBN₍₇₋₁₄₎) lead to a higher tumor-to-muscle uptake ratio (amounting to >30 at 100 min post injection) compared to ⁶⁴Cu-DMPTACN-βAla-βAla-BBN₍₇₋₁₄₎.

An interesting study performed by Bandari et al. [73] reported the first radiolabeled dual receptor/biomarker targeting agent based upon the GRPr and prostate-specific membrane antigen (PSMA), that had been validated in prostate cancer. They synthesized [DUPA-6-Ahx-(⁶⁴Cu-NODAGA)-5-Ava-BBN₍₇₋₁₄₎NH₂] and performed MicroPET and microCT imaging of GRPr positive PC-3 and PSMAr positive LNCaP tumor-bearing SCID mouse models (Fig. 3). Although the resulting images were not superior to similar monovalent or bivalent constructs previously reported, a single molecular imaging agent was synthesized and validated as potential agent for PSMA positive and GRP positive prostate cancer tumor identification [73].

4.4. Lutetium-177

Lutetium-177 (^{177}Lu) is a medium-energy β -emitter (E_{max} of 498.3 keV) and low-energy gamma emitter (E_{γ} max of 208 keV), which decays with a half-life of approximately 6.6 days [74]. The first paper describing ^{177}Lu as a potential diagnostic agent was published in 1968 for skeletal imaging purposes [75]. However, less than 10 papers were published on the development of ^{177}Lu -labeled radiopharmaceuticals in the last century whereas more than 500 publications have appeared in the last 20 years, demonstrating an explosive interest in and widespread applications of this radionuclide [76]. Despite being a late entrant into the nuclear medicine therapy arena, ^{177}Lu is expected to become one of the most widely used therapeutic radionuclides. This striking diffusion and exciting perspectives of ^{177}Lu may be attributed to (i) its ability, due to maximal tissue penetration of <3 mm of diameter, to cause localizing cytotoxic radiation in relatively small tumors as well as metastatic lesions and (ii) its scintigraphy imaging ability, allowed by low-energy γ -ray, and subsequent dosimetry with the same therapeutic compound [77]. Another worth mentioning advantage offered by ^{177}Lu , due to its relatively long half-life, is the possibility of shipment to sites distant from the reactor production facility with minimal decay loss [78].

Although ^{177}Lu is a lanthanide frequently used as a “no carrier added” isotope, a few studies have been reported in the use of this radioisotope coupled with various peptides, including BBN analogs. For the conjugation of ^{177}Lu with peptides resulting in kinetically inert with further inhibition of their *in vivo* transchelation activity, it is necessary the use of multidentate chelators that can be macrocyclic poliamino-carboxylate ligands, such as DOTA (1,4,7,10-tetraazacyclododecane- $\text{N},\text{N}',\text{N}'',\text{N}'''$ -tetraacetic acid) and DTPA (2-[bis[2-[bis(carboxymethyl)amino]ethyl]amino]acetic) or containing an asymmetrically substitute, such as DO3A (1,4,7-tris(carboxymethyl)10-(aminoethyl)-1,4,7,10-tetraazacyclododecaneOH) [79]. Several studies have been reported on the development of ^{177}Lu labeled BBN analogs for targeted imaging or therapy, and a summary focused on the papers with imaging studies can be found in Table 7.

Johnson et al. [80], using the PC-3 xenograft SCID mouse model evaluated the therapeutic benefit of combined GRP receptor targeted radiotherapy with chemotherapy. Scintigraphic images obtained 48 h post intravenous injection of ^{177}Lu -DOTA-8-Aoc-BBN₍₇₋₁₄₎NH₂ demonstrated selective *in vivo* GRP receptor targeting with rapid clearance of the non-receptor targeted radiolabeled material from non-target tissues and prolonged retention of the radiotherapeutic agent in receptor expressing tumor tissue. Zhang et al. performed biodistribution and scintigraphy studies in PC-3 athymic mice through intravenous injection of ^{177}Lu -DOTA-PEG4-BBN₍₇₋₁₄₎ and showed accumulation primarily in pancreas, kidney and tumor with a favorable tumor to liver ratio and a clear contrast from the background [81]. Similarly, a study performed by Lim et al. [82] describe the *in vitro* and *in vivo* biological characteristics of ^{177}Lu -DOTA-glu-BBN evaluated by biodistribution assays, SPECT/CT molecular imaging and radiotherapy studies with associated toxicities. The radiopeptide exhibited favorable pharmacokinetics with high tumor targeting and rapid blood clearance, which is conducive to both targeted radiotherapy and imaging. An image of data collected from SPECT can be found in Fig. 4. The potential of ^{177}Lu -AMBA as a γ -imaging and radiotherapeutic agent was evaluated by Maddalena et al. [83] in PC-3 as well

as in low GRPr-expressing models of prostate cancer (LNCaP and DU145). Results demonstrated uptake in all model systems, although PC-3 tumor uptake and retention of radioligand were about 10-fold higher than either DU145 or LNCaP. More importantly, the internalized dose of ^{177}Lu -AMBA in each of the tumor models was sufficient to reduce cell proliferation and tumor growth rate.

Using a different approach, Mendoza-Nava et al. [84] synthesized a ^{177}Lu -DOTA-dendrimer-folate-bombesin with gold nanoparticles in the dendritic cavity and demonstrated the potential use of this multifunctional system as an optical and nuclear imaging agent for breast tumors overexpressing GRP receptors. Also using a breast cancer xenograft model, Aranda-Lara et al. [85] assessed *in vitro* and *in vivo* properties of ^{177}Lu -folate- $\text{BBN}_{(1-14)}$. Micro-SPECT/CT imaging presented clearly visible tumors with high contrast and high retention after 24 h of intravenous injection. However, biodistribution studies results showed that, although ^{177}Lu -Folate- BBN heterovalent radiopharmaceutical enhanced the tumor radiation absorbed dose, kidney radiation absorbed doses were higher than in the tumors, demonstrating the need to further improve this class of radiolabeled peptides.

Based on the findings of fast metabolic degradation and blood clearance of BBN -based radiotracers, Valverde et al. [86] optimized bombesin-based radiotracers by synthesizing novel $\text{BBN}_{(7-14)}$ and $\text{BBN}_{(6-14)}$ conjugates and radiolabeling with ^{177}Lu . Through structural modifications of the peptide vector and amino acid substitutions as well as backbone modifications of the parent compound ^{177}Lu , the authors were able to identify, after a full evaluation of their *in vitro* and *in vivo* properties, a novel radiolabeled GRPr agonist with a high tumor uptake and a high tumor-to-kidney ratio. Despite the absence of imaging studies, several other groups have described biodistribution studies in normal mice as well as tumor-bearing mice using ^{177}Lu radio-labeled- BBN analogs, confirming its *in vivo* stability, excretion predominantly *via* urinary tract and efficacy in targeting GRPr positive tumors [87–89]. In the clinical settings, Bodei et al. [90] reported preliminary findings of a phase I study with 7 hormone refractory prostate cancer patients, in which ^{177}Lu -AMBA SPECT imaging showed lesions in five of the seven patients with high pancreatic uptake.

4.5. Other isotopes

Despite the majority of preclinical studies regarding radio-labeled BBN analogs for nuclear imaging makes use of the radioisotopes mentioned in the above sections, imaging properties of a few other radioisotopes have been evaluated. In this section, we will briefly describe examples of BBN radiolabeling with other PET and SPECT radioactive agents. A summary can be found in Table 8.

Indium-111 (^{111}In) is a widely used radioisotope used clinically. ^{111}In -oxine labeled autologous human leukocytes are used for evaluating patients suspected of having abscesses [79] whereas ^{111}In is the isotope used in Octreoscan, a radiolabeled somatostatin analog available in the market for scintigraphic localization of primary and metastatic neuroendocrine tumors overexpressing somatostatin receptors [91]. ^{111}In is an attractive isotope due to its adequate half-life of 67 h, emission of gamma energy of 247 keV and a type of disintegration producing an electron that is suitable for SPECT imaging [79]. HO et

al. [92] used DTPA as a chelator to conjugate ^{111}In to a bombesin analog ([Lys3, DTyr4]Bn₍₂₋₁₄₎) and performed biodistribution and imaging studies after tail vein injection into PC-3 cell xenograft models. Biodistribution studies revealed that ^{111}In -DTPA-(Lys3, DTyr4]Bn₍₂₋₁₄₎) accumulated in tumor, adrenal, pancreas, small intestine, and large intestine. Rapid blood clearance and excretion from the kidneys were also observed. MicroSPECT/CT showed uptake in the tumors at 8 and 24 h. High accumulation in the kidney, pancreas, and GI tract at 4, 8, 24, and 48 h [92].

Reynolds et al. [93] reported the ^{111}In radiolabeling of RM2 (D-Phe-Gln-Trp-Ala-Val-Gly-His-Sta-Leu-NH₂), which is an antagonist analog of BBN that has recently been shown to have improved uptake and retention in tumors as compared to agonistic-type GRPr-targeting ligands. DOTA was used as a chelator and RGD was also conjugated in the final complex along with ^{177}Lu for comparison results. MicroSPECT/CT images at 20 h post-injection produced high-quality, high-contrast, whole-body images with minimal tracer present in non-tumor tissues. Also, [RGD-Glu-[^{111}In -DO3A]-6-Ahx RM2] and [RGD-Glu-[^{177}Lu -DO3A]-6-Ahx-RM2] showed favorable pharmacokinetic and radiouptake profiles (Fig. 5) [93].

Among a number of positron-emitting nuclides, Fluorine-18 (^{18}F) appears to be one of the best candidates for labeling small molecules such as bioactive peptides due to its favorable physical and nuclear characteristics, including high positron decay ratio (97%), relatively short half-life (109.7 min), and low positron energy (maximum 0.635 MeV). The positron energy results in a short diffusion range (<2.4 mm) that favorably increases the resolution limits of the PET images [94]. Another major advantage is the possibility of ^{18}F production in large quantities with a cyclotron primarily by proton (^1H) irradiation of ^{18}O , a stable naturally occurring isotope of oxygen [95]. Since previously studies reported that full-length BBN present poor *in vivo* stability, Carlucci et al. [96] evaluated two full-length lanthionine-stabilized BBN analogs (named 4,7-lanthionine-BBN and 2,6-lanthionine-BBN) with respect to their ability to target GRPR and to their increased stability. NOTA was used as chelator because of its properties to stabilize the +2 charge of the Al $^{18}\text{F}^{2+}$ complex. microPET images and quantitative analysis showed that the average tumor-to-muscle ratios were favorable, demonstrating the possibility of utilization of lanthionine to stabilize BBN analogs [96].

Zhang et al. [97] radiolabeled [Lys3]bombesin ([Lys3]BBN) and aminocaproic acid-bombesin₍₇₋₁₄₎ (Aca-BBN₍₇₋₁₄₎) with N-succinimidyl-4- ^{18}F -fluorobenzoate (^{18}F -SFB) under slightly basic condition. Biodistribution studies and microPET imaging performed in PC-3 xenograft models showed excretion through kidneys and rapid blood clearance. For both compounds tested, tumor uptake and tumor-to-non-tumor ratio were higher for ^{18}F FB-[Lys3]BBN than for ^{18}F FB-Aca-BBN₍₇₋₁₄₎ and the latter obtained a high liver and gallbladder accumulation thus reducing the possibility of using this form of radiopeptide for detecting orthotopic prostate cancer [97].

One strategy that has been currently used to develop improved imaging probes is designing dual-targeting approaches that allow the radiopeptide to recognize more than one receptor, causing a synergistic effect. Based on the fact that androgen-independent prostate cancer

expresses both GRPR and integrin $\alpha v\beta 3$, Li et al. [98] developed a BBN-RGD peptide radiolabeled with N-Succinimidyl-4-18F-fluorobenzoate (^{18}F -SFB). MicroPET results revealed that, when compared with ^{18}F FB-BBN and ^{18}F FB-RGD, the PC-3 tumor uptake of ^{18}F FB-BBN-RGD was much higher than the sum of the monomeric tracers at all time points examined. ^{18}F FB-BBN-RGD also had the highest tumor-to-non-tumor confirming a synergistic effect [98]. Despite Fluorine-18 labeling chemistry had developed tremendously over the last decades, the major disadvantage of labeling peptides with this radionuclide is the laborious, time-consuming and challenging radiosynthesis and labeling strategies. Therefore, the development of easy and fast labeling techniques in biocompatible conditions is still needed.

Yttrium-86 (^{86}Y) is a non-pure positron emitter, in which 67% of its decays are accompanied by additional γ -rays with energies from 200 to 3000 keV that are emitted simultaneously with positron emissions and the subsequent annihilation photons. As a result, scatter and random events are increased during PET imaging and a large number of non-true coincidences generates a noisy background that decreases the contrast in reconstructed images [99]. Although ^{86}Y is not an ideal PET isotope, PET imaging with that radioisotope allows patient and compound-specific dose estimation for further therapies with radiopharmaceuticals labeled with ^{90}Y [100]. Erion et al. [101] performed PET/CT imaging with ^{86}Y radiolabeled DOTA-(Pro1, Tyr4)-bombesin(1–14) (MP2346) in PC-3 xenograft models and AR42J tumor bearing rats. ^{86}Y -MP2346 was stable, not susceptible to transchelation *in vivo* and obtained a favorable tumor concentration with low non-target tissue accumulation. This allowed for excellent delineation of the GRPR positive tumors in both mice and rats. A throughout review of radiolabeled bombesin-related reports from up to 2011 containing other radioisotopes not mentioned in this review can be found at [79].

Herein we presented an extensive and comparative report on the use of radiolabeled bombesin derivatives for molecular imaging of tumors overexpressing Bombesin-like binding receptors. In a broad sense, it is possible to ascertain the major role of nuclear molecular imaging, specifically PET and SPECT, in the visualization, characterization and measurement of tumor progression at the molecular and cellular levels. In both SPECT and PET, the intensity of the imaging signal is proportional to the amount of tracer and the ability to image physiological and functional processes, guided by the pharmacokinetics and biodistribution of the radiotracer, provides vital information not available from conventional imaging techniques. In this sense, the radiotracer plays a major role in the success of diagnostic accuracy optimization. An ideal radiotracer must specifically accumulate at the site of the tumor with a high signal-to-noise ratio. As such, the selection of both the isotope and the targeted agent is of major importance. An optimal isotope should emit photons with an energy between 100 and 300 keV (SPECT), have small decay branches for particle emission in order to minimize radiation damage, have a half-life that is at least $1.5 \times$ the duration of the test procedure and should be cost effective and readily available. An ideal targeting agent for a particular cancer must have high affinity and specificity to a molecular target that is specific to the cancer in question with consistently high expression levels per tumor cell throughout the natural progression of the disease and ideally does not alter this expression during therapy. Furthermore, an ideal radiotracer must be stable, have an appropriate circulation time *in vivo* and specifically accumulate in tumor tissue.

5. Conclusions and perspectives

The feasibility and advantage of using radiolabeled-bombesin peptides as agents for identification of tumors overexpressing gastrin-releasing peptides receptors is abundantly clear. Among the many bombesin peptides analogs already developed, a greater part of published studies make use of the truncated aminoacids relative to the 7th to 14th position (Gln-Trp-Ala-Val-Gly-His-Leu-Met-NH₂) of the full-length bombesin as it contains the peptide sequence responsible for specific binding. Radioisotopes can bind to BBN peptides *via* a diverse range of chelators, but it is important to acknowledge that the choice of chelator must play a significant role in isotope-BBN design since it can affect the affinity, biodistribution, and tumor uptake profile of the final radio-complex. Additionally, ^{99m}Tc appear to be the radioisotope of choice in the majority of the reports. However, this pattern is likely to change due to the increasing availability of PET imaging isotopes and its radiolabeling methods optimization, which coordinates with the tendency, in the clinical settings, of migrating to PET imaging technique because of its sensitive advantage when compared to SPECT techniques. It is also important to highlight the relevance of animal models, in the preclinical context, to mimic the physiopathology conditions of human tumors. In conclusion, radiolabeled bombesin peptides are promising candidates as markers of early detection of tumors and better cancer prognosis in the future. Nonetheless, further studies are necessary to bolster the correlation between preclinical studies in mouse tumor models with *in vivo* performance in cancer patients.

Acknowledgments

DMT is supported by the National Institute of General Medical Sciences (P20-GM103542-02) and the South Carolina Centers of Excellence program.

References

1. Ferro-Flores G, de F, Ramirez M, Melendez-Alafort L, Santos-Cuevas CL. Peptides for *in vivo* target-specific cancer imaging. *Mini Rev Med Chem.* 2010; 10:87–97. [PubMed: 20380643]
2. Zanzonico P. Principles of nuclear medicine imaging: planar, SPECT, PET, multi-modality, and autoradiography systems. *Radiat Res.* 2012; 177:349–364. doi: <http://dx.doi.org/10.1667/RR2577.1>. [PubMed: 22364319]
3. Santos-Cuevas CL, Ferro-Flores G, Arteaga de Murphy C, de Ramirez FM, Luna-Gutiérrez MA, Pedraza-López M, García-Becerra R, Ordaz-Rosado D. Design, preparation, *in vitro* and *in vivo* evaluation of ^{99m}Tc-N2S2-Tat(49–57)-bombesin: a target-specific hybrid radiopharmaceutical. *Int J Pharm.* 2009; 375:75–83. doi: <http://dx.doi.org/10.1016/j.ijpharm.2009.04.018>. [PubMed: 19393305]
4. Emonds KM, Swinnen JV, Mortelmans L, Mottaghy FM. Molecular imaging of prostate cancer. *Methods.* 2009; 48:193–199. doi: <http://dx.doi.org/10.1016/j.ymeth.2009.03.021>. [PubMed: 19362147]
5. de Barros AB, Tsourkas A, Saboury B, Cardoso VN, Alavi A. Emerging role of radiolabeled nanoparticles as an effective diagnostic technique. *EJNMMI Res.* 2012; 2:39. doi: <http://dx.doi.org/10.1186/2191-219X-2-39>. [PubMed: 22809406]
6. Beer AJ, Eiber M, Souvatzoglou M, Schwaiger M, Krause BJ. Radionuclide and hybrid imaging of recurrent prostate cancer. *Lancet Oncol.* 2011; 12:181–191. doi: [http://dx.doi.org/10.1016/S1470-2045\(10\)70103-0](http://dx.doi.org/10.1016/S1470-2045(10)70103-0). [PubMed: 20599424]

7. Higgins LJ, Pomper MG. The evolution of imaging in cancer: current state and future challenges. *Semin Oncol.* 2011; 38:3–15. doi: <http://dx.doi.org/10.1053/j.seminoncol.2010.11.010>. [PubMed: 21362512]
8. Schottelius M, Wester HJ. Molecular imaging targeting peptide receptors. *Methods.* 2009; 48:161–177. doi: <http://dx.doi.org/10.1016/j.ymeth.2009.03.012>. [PubMed: 19324088]
9. Fani M, Maecke HR. Radiopharmaceutical development of radiolabelled peptides. *Eur J Nucl Med Mol Imaging.* 2012; 39(Suppl. 1):11–30. doi: <http://dx.doi.org/10.1007/s00259-011-2001-z>.
10. Laverman P, Sosabowski JK, Boerman OC, Oyen WJG. Radiolabelled peptides for oncological diagnosis. *Eur J Nucl Med Mol Imaging.* 2012; 39(Suppl. 1):78–92. doi: <http://dx.doi.org/10.1007/s00259-011-2014-7>.
11. Sun, X., Li, Y., Liu, T., Li, Z., Zhang, X., Chen, X. Peptide-based imaging agents for cancer detection. *Adv Drug Deliv Rev.* 2016. doi: <http://dx.doi.org/10.1016/j.addr.2016.06.007>
12. Weiner RE, Thakur ML. Radiolabeled peptides in the diagnosis and therapy of oncological diseases. *Appl Radiat Isot Incl Data Instrum Methods Use Agric Ind Med.* 2002; 57:749–763.
13. Fani M, Maecke HR, Okarvi SM. Radiolabeled peptides: valuable tools for the detection and treatment of cancer. *Theranostics.* 2012; 2:481–501. doi: <http://dx.doi.org/10.7150/thno.4024>. [PubMed: 22737187]
14. Branco de Barros AL. Radiolabeled peptides as imaging probes for cancer diagnosis. *J Mol Pharm Org Process Res.* 2014; 2 doi: <http://dx.doi.org/10.4172/2329-9053.1000e115>.
15. Schroeder RPJ, van Weerden WM, Bangma C, Krenning EP, de Jong M. Peptide receptor imaging of prostate cancer with radiolabelled bombesin analogues. *Methods.* 2009; 48:200–204. doi: <http://dx.doi.org/10.1016/j.ymeth.2009.04.002>. [PubMed: 19398012]
16. Schroeder RPJ, de Visser M, van Weerden WM, de Ridder CMA, Reneman S, Melis M, Breeman WAP, Krenning EP, de Jong M. Androgen-regulated gastrin-releasing peptide receptor expression in androgen-dependent human prostate tumor xenografts. *Int J Cancer.* 2010; 126:2826–2834. doi: <http://dx.doi.org/10.1002/ijc.25000>. [PubMed: 19876914]
17. Ramos-Álvarez I, Moreno P, Mantey SA, Nakamura T, Nuche-Berenguer B, Moody TW, Coy DH, Jensen RT. Insights into bombesin receptors and ligands: highlighting recent advances. *Peptides.* 2015; 72:128–144. doi: <http://dx.doi.org/10.1016/j.peptides.2015.04.026>. [PubMed: 25976083]
18. Xiao C, Reitman ML. Bombesin-Like receptor 3: physiology of a functional orphan. *Trends Endocrinol Metab.* 2016; 27:603–605. doi: <http://dx.doi.org/10.1016/j.tem.2016.03.003>. [PubMed: 27055378]
19. Fuscaldi LL, de Barros ALB, de P Santos CR, de Souza CM, Cassali GD, de Oliveira MC, Fernandes SOA, Cardoso VN. Evaluation of the optimal LNCaP prostate tumour developmental stage to be assessed by ^{99m}Tc-HYNIC-¹⁸F-Ala-bombesin(7–14) in an experimental model. *J Radioanal Nucl Chem.* 2014; 300:801–807. doi: <http://dx.doi.org/10.1007/s10967-014-3040-2>.
20. Mansi R, Wang X, Forrer F, Waser B, Cescato R, Graham K, Borkowski S, Reubi JC, Maecke HR. Development of a potent DOTA-conjugated bombesin antagonist for targeting GRPr-positive tumours. *Eur J Nucl Med Mol Imaging.* 2011; 38:97–107. doi: <http://dx.doi.org/10.1007/s00259-010-1596-9>. [PubMed: 20717822]
21. Ferlay, FBJ., Soerjomataram, I., Ervik, M., Dikshit, R., Eser, S., Mathers, C., Rebelo, M., Parkin, DM., Forman, D. GLOBOCAN 2012. 0, cancer incidence and mortality worldwide: IARC CancerBase No. 11. Int Agency Res Cancer, Lyon. 2016. n.d.. <http://globocan.iarc.fr> Accessed 10 October 2016
22. de Barros ALB, das Mota LG, de Ferreira CA, Cardoso VN. Kit formulation for ^{99m}Tc-labeling of HYNIC-Ala-bombesin (7–14). *Appl Radiat Isot.* 2012; 70:2440–2445. doi: <http://dx.doi.org/10.1016/j.apradiso.2012.06.022>. [PubMed: 22871450]
23. Peterson JK, Houghton PJ. Integrating pharmacology and in vivo cancer models in preclinical and clinical drug development. *Eur J Cancer.* 2004; 40:837–844. doi: <http://dx.doi.org/10.1016/j.ejca.2004.01.003>. [PubMed: 15120039]
24. Talmadge JE, Singh RK, Fidler IJ, Raz A. Murine models to evaluate novel and conventional therapeutic strategies for cancer. *Am J Pathol.* 2007; 170:793–804. doi: <http://dx.doi.org/10.2353/ajpath.2007.060929>. [PubMed: 17322365]

25. Ni Y, Wang H, Chen F, Li J, DeKeyzer F, Feng Y, Yu J, Bosmans H, Marchal G. Tumor models and specific contrast agents for small animal imaging in oncology. *Methods*. 2009; 48:125–138. doi: <http://dx.doi.org/10.1016/j.ymeth.2009.03.014>. [PubMed: 19328231]
26. de Barros ALB, Mota LDG, Ferreira CDA, De Oliveira MC, De Góes AM, Cardoso VN. Bombesin derivative radiolabeled with technetium-99 m as agent for tumor identification. *Bioorg. Med Chem Lett*. 2010; 20:6182–6184. doi: <http://dx.doi.org/10.1016/j.bmcl.2010.08.124>.
27. de Barros ALB, das G Mota L, Soares DCF, Coelho MMA, Oliveira MC, Cardoso VN. Tumor bombesin analog loaded long-circulating and pH-sensitive liposomes as tool for tumor identification. *Bioorg Med Chem Lett*. 2011; 21:7373–7375. doi: <http://dx.doi.org/10.1016/j.bmcl.2011.10.016>. [PubMed: 22050889]
28. de Barros ALB, das Graças Mota L, de Aguiar Ferreira C, Corrêa NCR, de Góes MC, Cardoso VN. 99mTc-labeled bombesin analog for breast cancer identification. *J Radioanal Nucl Chem*. 2013; 295:2083–2090. doi: <http://dx.doi.org/10.1007/s10967-012-2331-8>.
29. Asabella AN, Cascini GL, Altini C, Paparella D, Notaristefano A, Rubini G. The Copper radioisotopes: a systematic review with special interest to 64 Cu. *Biomed Res Int*. 2014; 2014:1–9. doi: <http://dx.doi.org/10.1155/2014/786463>.
30. McQuade P, Rowland DJ, Lewis JS, Welch MJ. Positron-emitting isotopes produced on biomedical cyclotrons. *Curr Med Chem*. 2005; 12:807–818. doi: <http://dx.doi.org/10.2174/0929867053507397>. [PubMed: 15853713]
31. Rowland DJ, Cherry SR. Small-Animal preclinical nuclear medicine instrumentation and methodology. *Semin Nucl Med*. 2008; 38:209–222. doi: <http://dx.doi.org/10.1053/j.semnuclmed.2008.01.004>. [PubMed: 18396180]
32. Okarvi SM, Jammaz IA. Preparation and evaluation of bombesin peptide derivatives as potential tumor imaging agents: effects of structure and composition of amino acid sequence on in vitro and in vivo characteristics. *Nucl Med Biol*. 2012; 39:795–804. doi: <http://dx.doi.org/10.1016/j.nucmedbio.2012.01.002>. [PubMed: 22381782]
33. Banerjee S, Raghavan M, Pillai A, Ramamoorthy N. Evolution of Tc-99 M in Diagnostic Radiopharmaceuticals. 2001; XXXI:266–277.
34. Liolios CC, Fragogeorgi EA, Zikos C, Loudos G, Xanthopoulos S, Bouziotis P, Paravatou-Petsotas M, Livaniou E, Varvarigou AD, Sivolapenko GB. Structural modifications of 99mTc-labelled bombesin-like peptides for optimizing pharmacokinetics in prostate tumor targeting. *Int J Pharm*. 2012; 430:1–17. doi: <http://dx.doi.org/10.1016/j.ijpharm.2012.02.049>. [PubMed: 22459664]
35. Blok D, Feitsma HJJ, Kooy YMC, Welling MM, Ossendorp F, Vermeij P, Drijfhout JW. New chelation strategy allows for quick and clean 99mTc-labeling of synthetic peptides. *Nucl Med Biol*. 2004; 31:815–820. doi: <http://dx.doi.org/10.1016/j.nucmedbio.2004.02.009>. [PubMed: 15246374]
36. Baidoo KE, Lin KS, Zhan Y, Finley P, Scheffel U, Wagner HN. Design, synthesis, and initial evaluation of high-affinity technetium bombesin analogues. *Bioconjug Chem*. 1998; 9:218–225. doi: <http://dx.doi.org/10.1021/bc9701959>. [PubMed: 9548537]
37. Faintuch BL, Santos RLSR, Souza LFM, Hoffman TJ, Greeley M, Smith CJ. 99mTc-HYNIC-Bombesin (7–14)NH₂: radiochemical evaluation with Co-ligands EDDA (EDDA = ethylenediamine-N, N'-diacetic acid), tricine, and nicotinic acid. *Synth React Inorg Met Nano-Metal Chem*. 2005; 35:43–51. doi: <http://dx.doi.org/10.1081/SIM-200047545>.
38. Faintuch BL, Teodoro R, Duatti A, Muramoto E, Faintuch S, Smith CJ. Radiolabeled bombesin analogs for prostate cancer diagnosis: preclinical studies. *Nucl Med Biol*. 2008; 35:401–411. doi: <http://dx.doi.org/10.1016/j.nucmedbio.2008.02.005>. [PubMed: 18482677]
39. De Barros ALB, Mota LDG, Ferreira CDA, De Oliveira MC, De Góes AM, Cardoso VN. Bombesin derivative radiolabeled with technetium-99 m as agent for tumor identification. *Bioorg Med Chem Lett*. 2010; 20:6182–6184. doi: <http://dx.doi.org/10.1016/j.bmcl.2010.08.124>. [PubMed: 20850312]
40. Carlesso FN, Fuscaldi LL, Araújo RS, Teixeira CS, Oliveira MC, Fernandes SOA, Cassali GD, Reis DC, Barros ALB, Cardoso VN. Evaluation of 99mTc-HYNIC-BAla-bombesin(7–14) as an agent for pancreas tumor detection in mice. *Braz J Med Biol Res*. 2015; 48:923–928. [PubMed: 26445336]

41. Shi J, Jia B, Liu Z, Yang Z, Yu Z, Chen K, Chen X, Liu S, Wang F. ^{99m}Tc-labeled bombesin(7–14)NH₂ with favorable properties for SPECT imaging of colon cancer. *Bioconjug Chem.* 2008; 19:1170–1178. doi: <http://dx.doi.org/10.1021/bc700471z>. [PubMed: 18491928]
42. Ananias HJK, Yu Z, Hoving HD, Rosati S, Dierckx RA, Wang F, Yan Y, Chen X, Pruim J, Lub-de Hooge MN, Helfrich W, Elsinga PH, de Jong IJ. Application of ^{99m}Tc-technetium-HYNIC(tricine/TPPTS)-Aca-bombesin(7–14) SPECT/CT in prostate cancer patients. A first-in-man study. *Nucl Med Biol.* 2013; 40:933–938. doi: <http://dx.doi.org/10.1016/j.nucmedbio.2013.05.009>. [PubMed: 23891351]
43. Scopinaro F, De Vincentis G, Varvarigou AD, Laurenti C, Iori F, Remediani S, Chiarini S, Stella S, Nucleare M, La Sapienza U, I PU, Elena VR. ^{99m}Tc-bombesin detects prostate cancer and invasion of pelvic lymph nodes. *Eur J Nucl Med.* 2003; 30:2–6. doi: <http://dx.doi.org/10.1007/s00259-003-1261-7>.
44. Anger HO, Gottschalk A. Localization of brain tumors with the positron scintillation camera. *J Nucl Med.* 1963; 4:326–330. [PubMed: 14044114]
45. Fani M, Andre JP, Maecke HR. ⁶⁸Ga-PET: a powerful generator-based alternative to cyclotron-based PET radiopharmaceuticals. *Contrast Media Mol Imaging.* 2008; 3:67–77. doi: <http://dx.doi.org/10.1002/cmml.232>. [PubMed: 18383558]
46. Banerjee SR, Pomper MG. Clinical applications of gallium-68. *Appl Radiat Isot Incl Data, Instrum Methods Use Agric Ind Med.* 2013; 76:2–13. doi: <http://dx.doi.org/10.1016/j.apradiso.2013.01.039>.
47. Jamous M, Tamma ML, Gourni E, Waser B, Reubi JC, Maecke HR, Mansi R. PEG spacers of different length influence the biological profile of bombesin-based radiolabeled antagonists. *Nucl Med Biol.* 2014; 41:464–470. doi: <http://dx.doi.org/10.1016/j.nucmedbio.2014.03.014>. [PubMed: 24780298]
48. Schuhmacher J, Zhang H, Doll J, Macke HR, Matys R, Hauser H, Henze M, Haberkorn U, Eisenhut M. GRP receptor-targeted PET of a rat pancreas carcinoma xenograft in nude mice with a ⁶⁸Ga-labeled bombesin(6–14) analog. *J Nucl Med.* 2005; 46:691–699. [PubMed: 15809493]
49. Nock B, Nikolopoulou A, Chiotellis E, Loudos G, Maintas D, Reubi JC, Maina T. [^{99m}Tc]Demobesin 1, a novel potent bombesin analogue for GRP receptor-targeted tumour imaging. *Eur J Nucl Med Mol Imaging.* 2003; 30:247–258. doi: <http://dx.doi.org/10.1007/s00259-002-1040-x>. [PubMed: 12552343]
50. Smith CJ, Gali H, Sieckman GL, Higginbotham C, Volkert WA, Hoffman TJ. Radiochemical investigations of (^{99m}Tc)-N(3)S-X-BBN[7–14]NH(2): an in vitro/in vivo structure-activity relationship study where X = 0- 3- 5-, 8-, and 11-carbon tethering moieties. *Bioconjug Chem.* 2003; 14:93–102. doi: <http://dx.doi.org/10.1021/bc020034r>. [PubMed: 12526698]
51. La Bella R, Garcia-Garayoa E, Langer M, Blauenstein P, Beck-Sickinger AG, Schubiger PA. In vitro and in vivo evaluation of a ^{99m}Tc(I)-labeled bombesin analogue for imaging of gastrin releasing peptide receptor-positive tumors. *Nucl Med Biol.* 2002; 29:553–560. [PubMed: 12088725]
52. Zhang H, Schuhmacher J, Waser B, Wild D, Eisenhut M, Reubi JC, Maecke HR. DOTA-PESIN, a DOTA-conjugated bombesin derivative designed for the imaging and targeted radionuclide treatment of bombesin receptor-positive tumours. *Eur J Nucl Med Mol Imaging.* 2007; 34:1198–1208. doi: <http://dx.doi.org/10.1007/s00259-006-0347-4>. [PubMed: 17262215]
53. Liu Z, Niu G, Wang F, Chen X. (⁶⁸Ga)-labeled NOTA-RGD-BBN peptide for dual integrin and GRPR-targeted tumor imaging. *Eur J Nucl Med Mol Imaging.* 2009; 36:1483–1494. doi: <http://dx.doi.org/10.1007/s00259-009-1123-z>. [PubMed: 19360404]
54. Varasteh Z, Velikyan I, Lindeberg G, So J, Larhed M, Sandstro M, Selvaraju RK, Malmberg J, Tolmachev V, Orlova A. Synthesis and characterization of a high-Affinity NOTA-conjugated bombesin antagonist for GRPR-targeted tumor imaging. *Bioconjug Chem.* 2013; 24:1144–1153. [PubMed: 23763444]
55. Varasteh Z, Rosenström U, Velikyan I, Mitran B, Altai M, Honarvar H, Rosestedt M, Lindeberg G, Sörensen J, Larhed M, Tolmachev V, Orlova A. The effect of mini-PEG-based spacer length on binding and pharmacokinetic properties of a ⁶⁸Ga-labeled NOTA-conjugated antagonistic analog of bombesin. *Molecules.* 2014; 19:10455–10472. doi: <http://dx.doi.org/10.3390/molecules190710455>. [PubMed: 25036155]

56. So Hee Dho JCL. Development of a ⁶⁸Ga-labeled bombesin analog for gastrin-releasing peptide receptor-expressing prostate tumor imaging. *Adv Tech Biol Med.* 2015; 3:2–7. doi: <http://dx.doi.org/10.4172/2379-1764.1000135>.
57. Richter S, Wuest M, Bergman CN, Krieger S, Rogers BE, Wuest F. Metabolically stabilized ⁶⁸Ga-NOTA-Bombesin for PET imaging of prostate cancer and influence of protease inhibitor phosphoramidon. *Mol Pharm.* 2016; 13:1347–1357. doi: <http://dx.doi.org/10.1021/acs.molpharmaceut.5b00970>. [PubMed: 26973098]
58. Nock BA, Maina T, Krenning EP, de Jong M. To serve and protect: enzyme inhibitors as radiopeptide escorts promote tumor targeting. *J Nucl Med.* 2014; 55:121–127. doi: <http://dx.doi.org/10.2967/jnumed.113.129411>. [PubMed: 24287321]
59. Maecke HR, Hofmann M, Haberkorn U. (⁶⁸Ga)-labeled peptides in tumor imaging. *J Nucl Med.* 2005; 46(Suppl 1):172S–178S. [PubMed: 15653666]
60. Holland JP, Ferdani R, Anderson CJ, Lewis JS. Copper-64 radiopharmaceuticals for oncologic imaging. *PET Clin.* 2009; 4:49–67. doi: <http://dx.doi.org/10.1016/j.cpet.2009.04.013>. [PubMed: 27156895]
61. Anderson CJ, Ferdani R. Copper-64 radiopharmaceuticals for PET imaging of cancer: advances in preclinical and clinical research. *Cancer Biother Radiopharm.* 2009; 24:379–393. doi: <http://dx.doi.org/10.1089/cbr.2009.0674>. [PubMed: 19694573]
62. Gutfilen B, Valentini G. Radiopharmaceuticals in nuclear medicine: recent developments for SPECT and PET studies. *Biomed Res Int.* 2014; 2014 doi: <http://dx.doi.org/10.1155/2014/426892>.
63. Wadas TJ, Wong EH, Weisman GR, Anderson CJ. Copper chelation chemistry and its role in copper radiopharmaceuticals. *Curr Pharm Des.* 2007; 13:3–16. doi: <http://dx.doi.org/10.2174/138161207779313768>. [PubMed: 17266585]
64. Ramogida CF, Orvig C. Tumour targeting with radiometals for diagnosis and therapy. *Chem Commun.* 2013; 49:4720–4739. doi: <http://dx.doi.org/10.1039/c3cc41554f>.
65. Rogers BE, Bigott HM, McCarthy DW, Della Manna D, Kim J, Sharp TL, Welch MJ. MicroPET imaging of a gastrin-releasing peptide receptor-positive tumor in a mouse model of human prostate cancer using a ⁶⁴Cu-labeled bombesin analogue. *Bioconjug Chem.* 2003; 14:756–763. doi: <http://dx.doi.org/10.1021/bc034018l>. [PubMed: 12862428]
66. Rogers BE, Della Manna D, Safavy A. In vitro and in vivo evaluation of a ⁶⁴Cu-labeled polyethylene glycol-bombesin conjugate. *Cancer Biother. Radiopharm.* 2004; 19:25–34. doi: <http://dx.doi.org/10.1089/108497804773391649>.
67. Chen X, Park R, Hou Y, Tohme M, Shahinian AH, Bading JR, Conti PS. microPET and autoradiographic imaging of GRP receptor expression with ⁶⁴Cu-DOTA-[Lys3]bombesin in human prostate adenocarcinoma xenografts. *J Nucl Med.* 2004; 45:1390–1397. [PubMed: 15299066]
68. Yang YS, Zhang X, Xiong Z, Chen X. Comparative in vitro and in vivo evaluation of two ⁶⁴Cu-labeled bombesin analogs in a mouse model of human prostate adenocarcinoma. *Nucl Med Biol.* 2006; 33:371–380. doi: <http://dx.doi.org/10.1016/j.nucmedbio.2005.12.011>. [PubMed: 16631086]
69. Parry JJ, Kelly TS, Andrews R, Rogers BE. In vitro and in vivo evaluation of ⁶⁴Cu-labeled DOTA-linker-bombesin(7–14) analogues containing different amino acid linker moieties. *Bioconjug Chem.* 2007; 18:1110–1117. doi: <http://dx.doi.org/10.1021/bc0603788>. [PubMed: 17503761]
70. Nanda PK, Pandey U, Bottenus BN, Rold TL, Sieckman GL, Szczodroski AF, Hoffman TJ, Smith CJ. Bombesin analogues for gastrin-releasing peptide receptor imaging. *Nucl Med Biol.* 2012; 39:461–471. doi: <http://dx.doi.org/10.1016/j.nucmedbio.2011.10.009>. [PubMed: 22261143]
71. Craft JM, De Silva RA, Lears KA, Andrews R, Liang K, Achilefu S, Rogers BE. In vitro and in vivo evaluation of a ⁶⁴Cu-labeled NOTA-Bn-SCN-Aoc-bombesin analogue in gastrin-releasing peptide receptor expressing prostate cancer. *Nucl Med Biol.* 2012; 39:609–616. doi: <http://dx.doi.org/10.1016/j.nucmedbio.2011.12.004>. [PubMed: 22261146]
72. Bergmann R, Ruffani A, Graham B, Spiccia L, Steinbach J, Pietzsch J, Stephan H. Synthesis and radiopharmacological evaluation of ⁶⁴Cu-labeled bombesin analogs featuring a bis(2-pyridylmethyl)-1,4,7-triazacyclononane chelator. *Eur J Med Chem.* 2013; 70:434–446. doi: <http://dx.doi.org/10.1016/j.ejmech.2013.10.013>. [PubMed: 24184988]

73. Bandari RP, Jiang Z, Reynolds TS, Bernskoetter NE, Szczodroski AF, Bassuner KJ, Kirkpatrick DL, Rold TL, Sieckman GL, Hoffman TJ, Connors JP, Smith CJ. Synthesis and biological evaluation of copper-64 radiolabeled [DUPA-6-Ahx-(NODAGA)-5-Ava-BBN(7–14)NH₂], a novel bivalent targeting vector having affinity for two distinct biomarkers (GRPr/PSMA) of prostate cancer. *Nucl Med Biol*. 2014; 41:355–363. doi: <http://dx.doi.org/10.1016/j.nucmedbio.2014.01.001>. [PubMed: 24508213]
74. Pillai AMR, Knapp FFRJ. Evolving important role of lutetium-177 for therapeutic nuclear medicine. *Curr Radiopharm*. 2015; 8:78–85. [PubMed: 25771380]
75. O'Mara RE, McAfee JG, Subramanian G. Rare earth nuclides as potential agents for skeletal imaging. *J Nucl Med*. 1969; 10:49–51. [PubMed: 4978883]
76. Banerjee S, Pillai MRA, Knapp FF. Lutetium-177 therapeutic radiopharmaceuticals: linking chemistry, radiochemistry, and practical applications. *Chem Rev*. 2015; 115:2934–2974. doi: <http://dx.doi.org/10.1021/cr500171e>. [PubMed: 25865818]
77. Kam BLR, Teunissen JJM, Krenning EP, de Herder WW, Khan S, van Vliet EI, Kwekkeboom DJ. Lutetium-labelled peptides for therapy of neuroendocrine tumours. *Eur J Nucl Med Mol Imaging*. 2012; 39:103–112. doi: <http://dx.doi.org/10.1007/s00259-011-2039-y>.
78. Dash A, Pillai MRA, Knapp FF. Production of ¹⁷⁷Lu for targeted radionuclide therapy: available options. *Nucl Med Mol Imaging*. 2015; 49:85–107. 2010. doi: <http://dx.doi.org/10.1007/s13139-014-0315-z>. [PubMed: 26085854]
79. Sancho V, Di Florio A, Moody TW, Jensen RT. Bombesin receptor-mediated imaging and cytotoxicity: review and current status. *Curr Drug Deliv*. 2011; 8:79–134. doi: <http://dx.doi.org/10.2174/156720111793663624>. [PubMed: 21034419]
80. Johnson CV, Shelton T, Smith CJ, Ma L, Perry MC, Volkert WA, Hoffman TJ. Evaluation of combined (177)Lu-DOTA-8-AOC-BBN (7–14)NH₂ GRP receptor-targeted radiotherapy and chemotherapy in PC-3 human prostate tumor cell xenografted SCID mice. *Cancer Biother Radiopharm*. 2006; 21:155–166. doi: <http://dx.doi.org/10.1089/cbr.2006.21.155>. [PubMed: 16706636]
81. Zhang H, Schuhmacher J, Waser B, Wild D, Eisenhut M, Reubi JC, Maecke HR. DOTA-PESIN, a DOTA-conjugated bombesin derivative designed for the imaging and targeted radionuclide treatment of bombesin receptor-positive tumours. *Eur J Nucl Med Mol Imaging*. 2007; 34:1198–1208. doi: <http://dx.doi.org/10.1007/s00259-006-0347-4>. [PubMed: 17262215]
82. Lim JC, Cho EH, Kim JJ, Choi SM, Lee SY, Nam SS, Park UJ, Park SH. Preclinical pharmacokinetic, biodistribution, imaging and therapeutic efficacy of ¹⁷⁷Lu-Labeled glycosylated bombesin analogue for gastrin-releasing peptide receptor-positive prostate tumor targeting. *Nucl Med Biol*. 2015; 42:234–241. doi: <http://dx.doi.org/10.1016/j.nucmedbio.2014.10.008>. [PubMed: 25498002]
83. Maddalena ME, Fox J, Chen J, Feng W, Cagnolini A, Linder KE, Tweedle MF, Nunn AD, Lantry LE. ¹⁷⁷Lu-AMBA biodistribution, radiotherapeutic efficacy, imaging, and autoradiography in prostate cancer models with low GRP-R expression. *J Nucl Med*. 2009; 50:2017–2024. doi: <http://dx.doi.org/10.2967/jnumed.109.064444>. [PubMed: 19910427]
84. Mendoza-nava H, Ferro-flores G, Ramírez FDM, Ocampo-garcía B, Santos-cuevas C, Aranda-lara L, Azorín-vega E, Morales-avila E, Isaac-olivé K. Lu-dendrimer conjugated to folate and bombesin with gold nanoparticles in the dendritic cavity: a potential theranostic radiopharmaceutical. *Braz J Med Biol Res*. 2016 in press.
85. Aranda-Lara L, Ferro-Flores G, Azorín-Vega E, de María Ramírez F, Jiménez-Mancilla N, Ocampo-García B, Santos-Cuevas C, Isaac-Olivé K. Synthesis and evaluation of Lys1(α-γ-Folate)Lys3(177Lu-DOTA)-Bombesin (1–14) as a potential theranostic radiopharmaceutical for breast cancer. *Appl Radiat Isot*. 2016; 107:214–219. doi: <http://dx.doi.org/10.1016/j.apradiso.2015.10.030>. [PubMed: 26545016]
86. Valverde IE, Vomstein S, Mindt TL. Toward the optimization of bombesin-based radiotracers for tumor targeting. *J Med Chem*. 2016; 59:3867–3877. doi: <http://dx.doi.org/10.1021/acs.jmedchem.6b00025>. [PubMed: 27054526]
87. Hu F, Cutler CS, Hoffman T, Sieckman G, Volkert WA, Jurisson SS. Pm-149 DOTA bombesin analogs for potential radiotherapy. In vivo comparison with Sm-153 and Lu-177 labeled DO3A-amide-betaAla-BBN(7–14)NH₂. *Nucl Med Biol*. 2002; 29:423–430. [PubMed: 12031877]

88. Smith CJ, Gali H, Sieckman GL, Hayes DL, Owen NK, Mazuru DG, Volkert WA, Hoffman TJ. Radiochemical investigations of ¹⁷⁷Lu-DOTA-8-Aoc-BBN[7–14]NH₂: an in vitro/in vivo assessment of the targeting ability of this new radiopharmaceutical for PC-3 human prostate cancer cells. *Nucl Med Biol*. 2003; 30:101–109. [PubMed: 12623108]
89. Linder KE, Metcalfe E, Arunachalam T, Chen J, Eaton SM, Feng W, Fan H, Raju N, Cagnolini A, Lantry LE, Nunn AD, Swenson RE. In vitro and in vivo metabolism of Lu-AMBA, a GRP-receptor binding compound, and the synthesis and characterization of its metabolites. *Bioconjug Chem*. 2009; 20:1171–1178. doi: <http://dx.doi.org/10.1021/bc9000189>. [PubMed: 19480415]
90. Bodei L, Ferrari M, Nunn A, Llull J, Cremonesi M, Martano L, et al. ¹⁷⁷Lu-AMBA bombesin analogue in hormone refractory prostate cancer patients: a phase I escalation study with single-cycle administration. *Eur J Nucl Med Mol Imaging*. 2007; 34
91. van der Lely AJ, de Herder WW, Krenning EP, Kwekkeboom DJ. Octreoscan radioreceptor imaging. *Endocrine*. 2003; 20:307–311. doi: <http://dx.doi.org/10.1385/ENDO:20:3:307>. [PubMed: 12721512]
92. Ho CL, Chen LC, Lee WC, Chiu SP, Hsu WC, Wu YH, Yeh CH, Stabin MG, Jan ML, Lin WJ, Lee TW, Chang CH. Receptor-binding, biodistribution, dosimetry, micro-SPECT/CT imaging of ¹¹¹In-[DTPA1, Lys3, Tyr4]-bombesin analog in human prostate tumor-bearing mice. *Cancer Biother Radiopharm*. 2016; 24:435–443. n.d.
93. Stott Reynolds TJ, Schehr R, Liu D, Xu J, Miao Y, Hoffman TJ, Rold TL, Lewis MR, Smith CJ. Characterization and evaluation of DOTA-conjugated bombesin/RGD-antagonists for prostate cancer tumor imaging and therapy. *Nucl Med Biol*. 2015; 42:99–108. doi: <http://dx.doi.org/10.1016/j.nucmedbio.2014.10.002>. [PubMed: 25459113]
94. Okarvi SM. Recent progress in fluorine-18 labelled peptide radiopharmaceuticals. *Eur J Nucl Med*. 2001; 28:929–938. [PubMed: 11504093]
95. Jacobson O, Kiesewetter DO, Chen X. Fluorine-18 radiochemistry labeling strategies and synthetic routes. *Bioconjug Chem*. 2015; 26:1–18. doi: <http://dx.doi.org/10.1021/bc500475e>. [PubMed: 25473848]
96. Carlucci G, Kuipers A, Ananias HJK, De Paula Faria D, Dierckx RAJO, Helfrich W, Rink R, Moll GN, De Jong IJ, Elsinga PH. GRPR-selective PET imaging of prostate cancer using [¹⁸F]-lanthionine-bombesin analogs. *Peptides*. 2015; 67:45–54. doi: <http://dx.doi.org/10.1016/j.peptides.2015.03.004>. [PubMed: 25797109]
97. Zhang X, Cai W, Cao F, Schreibmann E, Wu Y, Wu JC, Xing L, Chen X. ¹⁸F-labeled bombesin analogs for targeting GRP receptor-expressing prostate cancer. *J Nucl Med*. 2006; 47:492–501. [PubMed: 16513619]
98. Li ZB, Wu Z, Chen K, Ryu EK, Chen X. ¹⁸F-labeled BBN-RGD heterodimer for prostate cancer imaging. *J Nucl Med*. 2008; 49:453–461. doi: <http://dx.doi.org/10.2967/jnumed.107.048009>. [PubMed: 18287274]
99. Buchholz HG, Herzog H, Förster GJ, Reber H, Nickel O, Rösch F, Bartenstein P. PET imaging with yttrium-86: comparison of phantom measurements acquired with different PET scanners before and after applying background subtraction. *Eur J Nucl Med Mol Imaging*. 2003; 30:716–720. doi: <http://dx.doi.org/10.1007/s00259-002-1112-y>. [PubMed: 12605273]
100. Herzog H, Rosch F, Stocklin G, Lueders C, Qaim SM, Feinendegen LE. Measurement of pharmacokinetics of yttrium-86 radiopharmaceuticals with PET and radiation dose calculation of analogous yttrium-90 radiotherapeutics. *J Nucl Med*. 1993; 34:2222–2226. [PubMed: 8254415]
101. Biddlecombe GB, Rogers BE, de Visser M, Parry JJ, de Jong M, Erion JL, Lewis JS. Molecular imaging of gastrin-releasing peptide receptor-positive tumors in mice using ⁶⁴Cu- and ⁸⁶Y-DOTA-(Pro1, Tyr4)-bombesin(1–14). *Bioconjug Chem*. 2007; 18:724–730. doi: <http://dx.doi.org/10.1021/bc060281i>. [PubMed: 17378600]
102. Marostica LL, de Barros ALB, Silva JO, Lopes SCA, Salgado BS, Chondrogiannis S, Rubello D, Cassali GD, Schenkel EP, Cardoso VN, Simoes CMO, Oliveira MC. Feasibility study with ^{99m}Tc-HYNIC-betaAla-bombesin(7–14) as an agent to early visualization of lung tumour cells in nude mice. *Nucl Med Commun*. 2016; 37:372–376. doi: <http://dx.doi.org/10.1097/MNM.0000000000000449>. [PubMed: 26629771]
103. Breeman WAP, de Jong M, Erion JL, Bugaj JE, Srinivasan A, Bernard BF, Kwekkeboom DJ, Visser TJ, Krenning EP. Preclinical comparison of (¹¹¹In)-labeled DTPA- or DOTA-bombesin

- analogs for receptor-targeted scintigraphy and radionuclide therapy. *J Nucl Med.* 2002; 43:1650–1656. <http://jnm.snmjournals.org/content/43/12/1650>. Abstract. [PubMed: 12468515]
104. Faintuch BL, Teodoro R, Duatti A, Muramoto E, Faintuch S, Smith CJ. Radiolabeled bombesin analogs for prostate cancer diagnosis: preclinical studies. *Nucl Med Biol.* 2008; 35:401–411. doi: <http://dx.doi.org/10.1016/j.nucmedbio.2008.02.005>. [PubMed: 18482677]
105. Pujatti PB, Foster JM, Finucane C, Hudson CD, Burnet JC, Pasqualoto KFM, Mengatti J, Mather SJ, de Araújo EB, Sosabowski JK. Evaluation and comparison of a new DOTA and DTPA-bombesin agonist in vitro and in vivo in low and high GRPR expressing prostate and breast tumor models. *Appl Radiat Isot.* 2015; 96:91–101. doi: <http://dx.doi.org/10.1016/j.apradiso.2014.11.006>. [PubMed: 25479439]
106. Fuscaldi LL, de Barros ALB, de P Santos CR, de Oliveira MC, Fernandes SOA, Cardoso VN. Feasibility of the ^{99m}Tc-HYNIC-(Ala-bombesin(7–14)) for detection of LNCaP prostate tumour in experimental model. *J Radioanal Nucl Chem.* 2015; 305:379–386. doi: <http://dx.doi.org/10.1007/s10967-015-4030-8>.

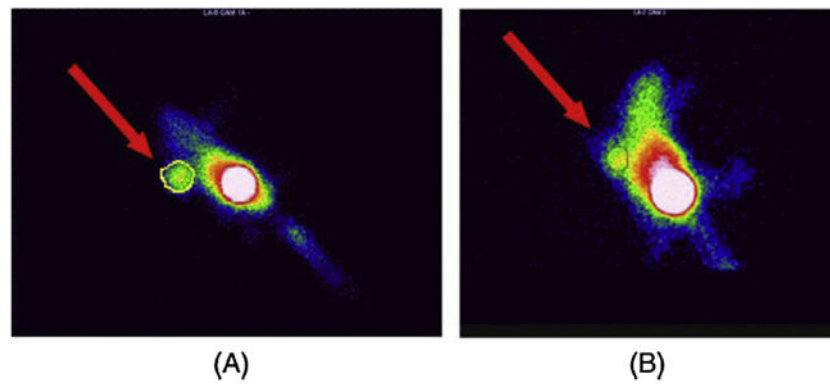


Fig. 1. Images of mice bearing PC-3 tumor xenografts 1.5 h after injection of ^{99m}Tc -HYNIC-BBN: unblocked tumor (A) and blocked tumor with 100 μg of HYNIC-BBN (B). Reproduced with permission from [38].

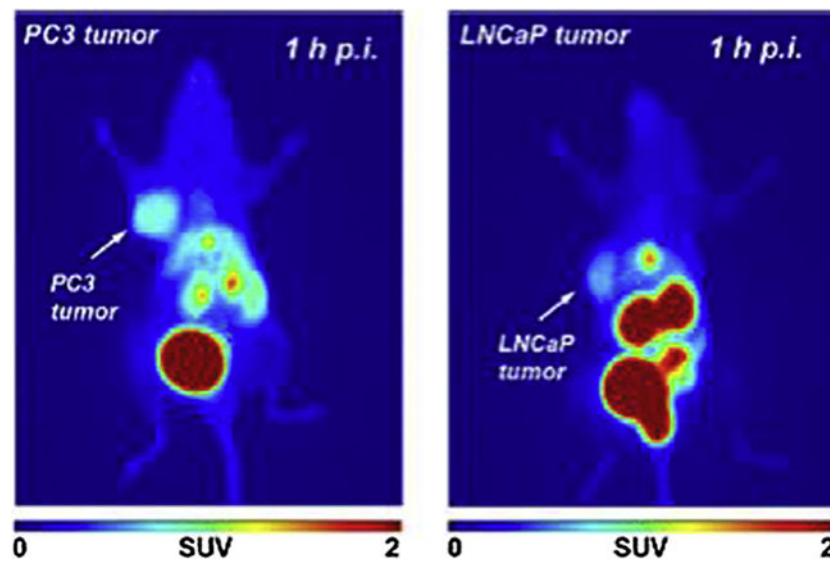


Fig. 2. Representative PET images (maximum intensity projection) of PC-3 (left) and LNCaP tumor-bearing BALB/c mouse (right) at 60 min after injection of ^{68}Ga -NOTA-BBN2. Adapted with permission from [57]

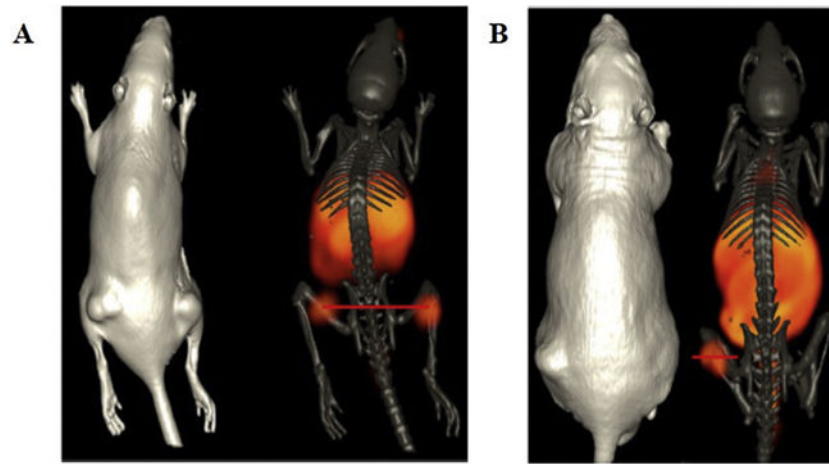


Fig. 3. (A) Maximum intensity microPET tumor and microCT skeletal fusion coronal whole body image of a PC-3 tumor-bearing SCID mouse at 18 h after tail vein injection of [DUPA-6-Ahx-(^{64}Cu -NODAGA)-5-Ava-BBN₍₇₋₁₄₎NH₂]. (B) Maximum intensity microPET tumor and microCT skeletal fusion coronal whole body image of an LNCaP tumor-bearing nude mouse at 18 h after tail vein injection of [DUPA-6-Ahx-(^{64}Cu -NODAGA)-5-Ava-BBN₍₇₋₁₄₎NH₂].

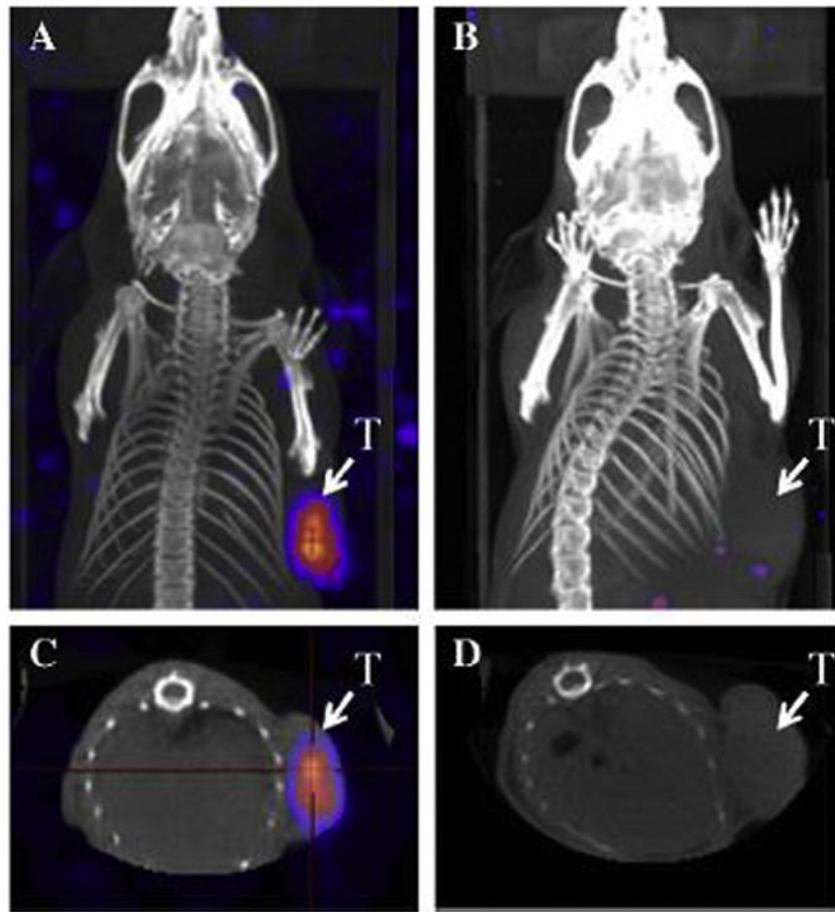


Fig. 4. SPECT images of PC-3 tumor-bearing mice acquired 1 h after the injection of 27.75 MBq of ^{177}Lu -DOTA-gluBBN (A–D). For a blocking study, 10^{-7} mol of the unlabeled peptide was co-injected (B, D). The image planes are as follows: coronal for (A) and (B), and transaxial for (C) and (D).

Reproduced with permission from [82].

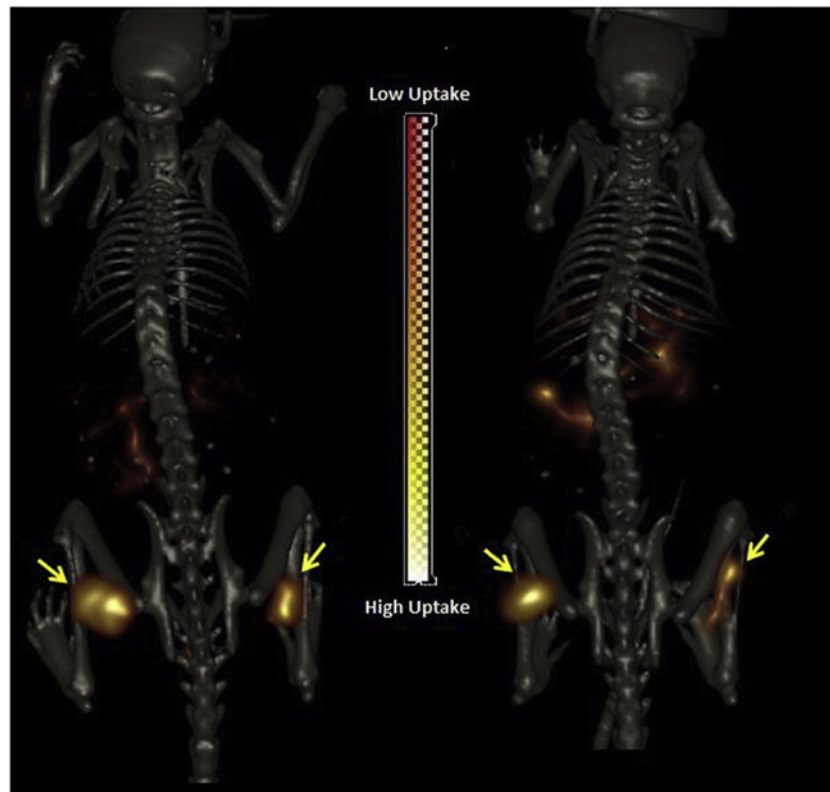


Fig. 5. Maximum intensity microSPECT tumor and microCT skeletal fusion coronal, whole-body images of PC-3 tumor-bearing SCID mice at 20 h post-tail vein injection of [RGD-Glu-[¹¹¹InDO3A]-6-Ahx-RM2] (left) and [RGD-Glu-[¹⁷⁷Lu-DO3A]-6-Ahx-RM2] (right). Tumors are indicated by arrows. Reproduced with permission from [93].

Table 1

Peptide receptors overexpressed on tumor cells surface.

Peptides	Cancers with upregulated peptide receptor expression
α -melanocyte stimulating hormone	Melanoma
Bombesin/Gastrin-releasing peptide	Breast cancer; Colon cancer; Gastric cancer; Glioblastoma; Pancreatic cancer; Prostate cancer; Small cell lung cancer
Cholecystokinin-B	Gastrointestinal cancer; Ovarian cancer; Small cell lung cancer; Thyroid cancer
Epidermal growth factor	Breast cancer
Neurotensin	Colon cancer; Meningioma; Pancreatic cancer; Prostate cancer; Small cell lung cancer
Somatostatin	Breast cancer; Lymphoma; Neuroendocrine cancer; Small cell lung cancer
Substance P	Breast cancer; Glial cancer; Thyroid cancer
Vasoactive Intestinal Peptide	Bladder cancer; Breast cancer; Colon cancer; Epithelial cancer; non-Small cell lung cancer; Pancreatic cancer; Prostate cancer; Ovarian cancer

Author Manuscript

Author Manuscript

Author Manuscript

Author Manuscript

Table 2

Amino acid residues sequence of Bombesin (BBN) and Gastrin-Releasing Peptide (GRP).

BBN	-----EQRLGNQWAVGHLM-NH ₂
GRP	---APVSVGGTVLAKMYPRGNHWAVGHLM-NH ₂

Author Manuscript

Author Manuscript

Author Manuscript

Author Manuscript

Table 3

Oncological animal models for the assessment of radiolabeled BBN derivatives as imaging probes for BBN receptors overexpressing tumors.

Animal	Tumor cells line	Type/Site of tumor cells inoculation	Refs.
Female Swiss mice	Ehrlich (murine breast cancer)	Allograft/Ectopic (thigh)	[26,27]
Female nude mice	MDA-MB-231 (human breast cancer)	Xenograft/Ectopic (thigh)	[28]
Female nude mice	HT-29 (human colorectal cancer)	Xenograft/Ectopic (upper flank)	[41]
Female nude mice	A549 (human lung cancer)	Xenograft/Ectopic (thigh)	[102]
Male rats	AR42J (rat pancreas cancer)	Allograft/Ectopic (thigh)	[101,103]
Male nude mice	Capan-1 (human pancreas cancer)	Xenograft/Ectopic (upper flank)	[40]
Male nude mice Male SCID mice	PC3 (human prostate cancer)	Xenograft/Ectopic (upper flank; lower flank)	[104,105]
Male nude mice	LNCaP (human prostate cancer)	Xenograft/Ectopic (upper flank)	[19,20,106]

Table 4*In vivo* imaging studies with Tc-99 m radiolabeled BBN derivatives.

Peptide	Linker	Animal Model	Reference
[Lys3]BBN	Pm-DADT or Hx-DADT	Normal CD-1 mice	[36]
BBN ₍₇₋₁₄₎	N(PNP6)-Cys HYNIC-β-Ala	PC-3 tumor-bearing nude mice	[38]
		PC-3 tumor-bearing nude mice	[38]
		Ehrlich tumor-bearing Swiss mice	[39]
		Capan-1 tumor-bearing nude mice	[40]
		MDA-MB-231 tumor-bearing athymic nude mice	[28]
		HT-29 tumor-bearing BALB/c nude mice	[41]
BBN ₍₂₋₁₄₎	Gly-Gly-Cys-[spacer] ₃ (arginine or ornithine)	PC-3 tumor-bearing SCID mice	[34]

Author Manuscript

Author Manuscript

Author Manuscript

Author Manuscript

Table 5*In vivo* imaging studies with Ga-68 radiolabeled BBN derivatives.

Peptide	Linker	Animal Model	Reference
BBN ₍₇₋₁₄₎	DOTA-PEG ₄	PC-3 tumor-bearing athymic nude mice	[52]
	DOTA-glu	PC-3 tumor-bearing balb/c nude mice	[56]
BBN ₍₇₋₁₄₎ -RGD	NOTA	PC-3 or MDA-MB-435 tumor-bearing athymic nude mice	[53]
[D-Phe ⁶ ,Sta ¹³ ,Leu ¹⁴]-bombesin ⁶⁻¹⁴ [6-14]	NOTA-PEG ₂	PC-3 tumor-bearing BALB/c nu/nu mice	[54]
	NOTA-PEG _n	PC-3 or BT-474 tumor-bearing BALB/c nu/nu mice	[55]
[DTyr ⁶ , β-Ala ¹¹ , Thi ¹³ , Nle ¹⁴] BBN ₍₆₋₁₄₎	DOTA-PEG ₂	AR42J tumor bearing Swiss CD1 <i>nu/nu</i> mice	[48]
BBN2	NOTA	PC-3 or LNCaP tumor-bearing BALB/c nude mice	[57]

Author Manuscript

Author Manuscript

Author Manuscript

Author Manuscript

Table 6*In vivo* imaging studies with ⁶⁴Cu radiolabeled BBN derivatives.

Peptide	Linker	Animal Model	Reference
BBN ₍₇₋₁₄₎	DOTA-Aoc	PC-3 tumor-bearing athymic nude mice	[65]
	DOTA-PEG	PC-3 tumor-bearing athymic nude mice	[66]
	DOTA or DOTA-X (X = GGG, GSG or GSS)	PC-3 tumor-bearing SCID mice	[69]
	NOTA-Bn-SCN-Aoc	PC-3 tumor-bearing SCID mice	[71]
	DMPTACN—COOH	PC-3 tumor-bearing NMRI nu/nu mice	[72]
	NODAGA-5-Ava	PC-3 tumor-bearing SCID mice	[73]
BBN ₍₇₋₁₄₎ or [Lys ³]BBN	DOTA OR DOTA-Aca	PC-3 tumor-bearing athymic nude mice or 22Rv1 tumor athymic nude mice	[68]
[Lys ³]BBN	DOTA	PC-3 or CWR22 tumor-bearing athymic nude mice	[67]
BBN ₍₆₋₁₃₎	NOTA-6-Ahx, NOTA-8-Aoc or NOTA-9-Anc	PC-3 tumor-bearing SCID mice	[70]

Table 7*In vivo* imaging studies with ^{177}Lu radiolabeled BBN derivatives.

Peptide	Linker	Animal Model	Reference
BBN ₍₇₋₁₄₎	DOTA-8-Aoc	PC-3 tumor-bearing SCID Mice	[80]
	DOTA-PEG ₄	PC-3 tumor-bearing athymic nude mice	[81]
	DO3A-CH ₂ CO-G-4-aminobenzoyl [AMBA]	PC-3, LNCap and DU145 tumor-bearing nude mice (separately)	[83]
	DOTA	T47D tumor-bearing mice	[84]
	DOTA-Lys(glucose)-4 aminobenzoic acid	PC-3 tumor-bearing SCID Mice	[82]
BBN ₍₇₋₁₄₎ and BBN ₍₆₋₁₄₎ derivatives	DOTA-PEG ₄	PC3 and AR42J tumor-bearing mice	[86]
BBN ₍₁₋₁₄₎	DOTA	T47D tumor-bearing mice	[85]

Author Manuscript

Author Manuscript

Author Manuscript

Author Manuscript

Table 8*In vivo* imaging studies BBN derivatives radiolabeled with ^{18}F , ^{111}In and ^{86}Y .

Radioisotope	Peptide	Linker	Animal Model	Reference
^{111}In	RM2-RGD	DOTA	PC-3 tumor-bearing SCID mice	[93]
	[Lys ³ , Tyr ⁴]Bn ₍₂₋₁₄₎	DTPA	PC-3 tumor-bearing SCID mice	[92]
^{18}F	BBN	NOTA-4,7-lanthionine-BBN and NOTA-2,6-lanthionine-BBN	PC-3 tumor-bearing athymic nude mice	[96]
	[Lys ³]BBN and Aca-BBN ₍₇₋₁₄₎	SFB	PC-3 and DU-145 tumor-bearing athymic nude mice	[97]
	BBN ₍₇₋₁₄₎ -RGD	SFB	PC-3 and DU-145 tumor-bearing athymic nude mice	[98]
^{86}Y	MP2346	DOTA	PC-3 tumor-bearing athymic mice and AR42J tumor-bearing rats	[101]